Journal of Applied Ichthyology

WILEY

RESEARCH ARTICLE OPEN ACCESS

Oocyte Development and Fecundity Strategy in Cage-Reared Pearlspot, *Etroplus suratensis* (Cichlidae): A Histological and Statistical Approach

Mohammad Saddam Hussain[1,2] | Mahadevan Harikrishnan[2] | Betsee Thomas[2] | P. V. Keerthana[3] | A. R. Nikhila Khanna[2] | Haritha Haridas[2] | Dinesh Yadav[4]

[1]Directorate of Agricultural Research, Nepal Agricultural Research Council, Lumbini, Khajura, Banke, Nepal | [2]School of Industrial Fisheries, Cochin University of Science and Technology, Kochi, Kerala 682016, India | [3]National Centre for Aquatic Animal Health, Cochin University of Science and Technology, Kochi, Kerala 682016, India | [4]National Animal Science Research Institute, Nepal Agricultural Research Council, Khumaltar, Lalitpur, Nepal

Correspondence: Mohammad Saddam Hussain (mshussain.np@gmail.com)

Received: 21 June 2025 | **Revised:** 22 January 2026 | **Accepted:** 2 February 2026

Academic Editor: Gournaga Biswas

Keywords: asynchronous oocyte development | *Etroplus suratensis* | indeterminate fecundity | oocyte atresia | oocyte recruitment

ABSTRACT

The progression of oocyte development and patterns of oocyte recruitment are key indicators of reproductive strategy in fishes. The present study examines, for the first time, the fecundity strategy of cage-reared *Etroplus suratensis* in Vembanad Lake using four indicators: (a) the oocyte size frequency distribution across ovarian reproductive phases and sampling months; (b) the proportional distribution of the oocyte developmental stages across each ovarian reproductive phase; (c) seasonal trends in the mean diameter of advanced vitellogenic oocytes; and (d) the seasonal incidence of oocyte atresia. The samples were collected monthly from October 2023 to September 2024, with 202 ovaries categorized by macroscopic observation into various ovarian reproductive phases. From these, 54 ovaries representing all ovarian reproductive phases were selected for histological examination and image analysis techniques. Histological examination identified seven distinct oocyte development stages in addition to postovulatory follicles and atretic oocytes. The oocyte size distribution revealed asynchronous oocyte development and continuous secondary growth, with no distinct separation between previtellogenic and vitellogenic oocytes. Gaussian mixture model analysis identified five distinct oocyte size clusters corresponding to successive developmental stages, confirming the presence of multiple cohorts. Logistic regression showed that the size at which 50% of oocytes recruited into vitellogenesis decreased across spawning-capable phases, reflecting rapid oocyte recruitment during repeated spawning events. A seasonal decline in the mean diameter of advanced vitellogenic oocytes was evident during the spawning season, indicating the continuous replenishment of oocytes within the advanced vitellogenic pool. A relatively stable proportion of cortical alveolar and vitellogenic oocytes during the spawning season suggests continuous recruitment of oocytes into the vitellogenic pool through *de novo vitellogenesis*. Furthermore, an increased occurrence of atretic oocytes was noticeable towards the end of the spawning season (i.e., August to October), reflecting a common strategy in species with indeterminate fecundity to reabsorb surplus oocytes. These findings demonstrate that *E. suratensis* exhibits asynchronous oocyte development, continuous oocyte recruitment and batch spawning with an indeterminate fecundity pattern. This reproductive strategy observed supports prolonged spawning activity and provides important implications for brood stock management and seed production in estuarine cage culture systems.

1 | Introduction

Etroplus suratensis, often known as pearlspot or green chromide, belongs to the Cichlidae family and is frequently found in both freshwater and estuarine habitats across Sri Lanka and India [1–3]. This economically significant food fish has a high market price because of its delicate flavour and reputation as an ornamental fish [3]. Pearlspot has made a major contribution to capture fisheries over the past several decades in the southwestern coastal backwaters of Kerala.

The reproductive cycle of female fish is closely associated with sequential stages of ovarian development, which results in physiological and morphological changes in the ovary, including the growth and differentiation of oocytes [4, 5]. Therefore, knowledge of oocyte development is necessary for determining the spawning season, size at maturity, spawning pattern and oocyte recruitment phenomena. Comprehensive knowledge of ovarian organization, oocyte development patterns and the type of fecundity regulation strategy (i.e., indeterminate or determinate fecundity) is an effective tool for quantifying the reproductive potential of any fish species to understand population dynamics and develop management models [6–10].

The pearlspot is a commercially significant species for capture fisheries in Vembanad Lake. It is an iteroparous and gonochoristic species that reproduces through external fertilization and provides parental care [11, 12]. Furthermore, this species exhibits a protracted spawning season, a characteristic typical of warm water habitats. However, the timing of spawning varies across its natural habitat [13]. In the context of Vembanad Lake, the peak spawning season was observed during the onset of the southwest monsoon (i.e., May–August) and the northeast monsoon season (i.e., November–January) [14]. The estimated size at first maturity in Vembanad Lake ranges from 169 to 200 mm for females and 167 to 195 mm for males and is typically reached after one year of age [14, 15]. Earlier research on pearlspot has primarily addressed age, growth, mortality and feeding habits, with limited emphasis on reproductive biology. Apart from recent studies on captive breeding and seed production in raceway tanks and fibre reinforced tanks [15], most investigations in Vembanad Lake and other estuaries have relied on macroscopic gonadal staging, seasonal spawning patterns and general fecundity estimates [14, 16]. While these approaches provide useful insights, detailed histological validation of ovarian organization, oocyte development dynamics and fecundity regulation remains limited, particularly under cage culture conditions. Previous studies based on the macroscopic observations of gonads and whole-mount oocyte size frequency distribution across ovarian maturity stages indirectly suggest that this species is an asynchronous and multiple-batch spawner with indeterminate fecundity [16]. However, histologically based evidence on oocyte size frequency distribution, cohort analysis and seasonal changes in advanced vitellogenic oocyte size, and the occurrence of atresia remains unreported. Moreover, information on continuous oocyte recruitment, batch-spawning dynamics and the replenishment of vitellogenic oocytes following spawning events is scarce.

In addition, most previous studies have focused on wild-caught populations, with little emphasis on cage-reared fish, despite the growing importance of cage culture for pearlspot in estuarine systems. Cage culture offers a practical approach for maintaining broodstock under seminatural estuarine conditions, where natural environmental cues are retained while controlled feeding and stocking densities reduce stress and promote gonadal development. This method supports a sustainable strategy for broodstock management and seed production, thereby reducing dependence on wild populations and contributing to both conservation and the expansion of aquaculture. Its effectiveness for broodstock maintenance and seed rearing in pearlspot has been documented in seed production protocols [17]. More recently, community-based cage breeding models have demonstrated frequent spawning and high fry production from broodstock maintained in floating net cages, with larval rearing supported by a recirculatory aquaculture system [18].

Histological analysis provides precise information on oocyte developmental stages that cannot be reliably identified through external or macroscopic observations alone and remains the most accurate method for assessing spawning readiness, oocyte recruitment patterns and spawning strategies [19]. However, detailed histological characterization across ovarian reproductive phases remains limited for pearlspot. The insights gained from this study can help fish farmers or hatchery managers to optimize spawning intervals, modification of external environment, reduce handling stress and improve seed production efficiency. Since many cichlid species share similar reproductive traits, including parental care, prolonged spawning seasons and asynchronous oocyte development, the histological framework developed here can also be applied to other cichlids for broodstock management, breeding schedule optimization and reproductive performance assessment, respectively.

This study aims, for the first time, to identify the fecundity type of pearlspot in Vembanad Lake by examining oocyte development and recruitment patterns, in order to test the hypothesis that pearlspot exhibits indeterminate fecundity. For this purpose, histological analysis techniques were employed to assess oocyte development [20, 21]. The study is based on four key criteria outlined in Refs. [5, 22]: (a) seasonal and stage-specific variations in oocyte size frequency distribution; (b) variation in the distribution of oocyte developmental stages throughout the spawning season in spawning-capable individuals; (c) seasonal trend in the average diameter of oocytes at advanced vitellogenic stages in spawning-capable individuals; and (d) the occurrence of atresia across the spawning season.

2 | Materials and Methods

2.1 | Study Site and Sample Collection

A total of 202 females of pearlspot at different maturity stages were collected monthly between October 2023 and September 2024 from cage culture systems installed in Vembanad Lake, Kerala, India. Each cage ($4 \times 3 \times 1.5$ m; L × B × H) was stocked with 500 fish and provided with floating feed containing 30% crude protein (2 mm pellet size). The cages were positioned in open estuarine waters with regular tidal exchange, thereby exposing the fish to natural environmental cues such as temperature, salinity and photoperiod, while maintaining seminatural

culture conditions. Random samples were collected from multiple cages and transported on ice to the laboratory for morphometric measurements and gonadal examination. Water quality parameters, including pH, temperature and salinity, were recorded monthly. A digital pH metre (Model HI98107) was used to measure pH, salinity with a refractometer (model: HHTEC, RHW-80) and temperature with a digital thermometer.

Water temperature in the estuarine cage culture system ranged from 24°C to 34°C, salinity varied between 1 and 20 ppt, and pH ranged from 6.3 to 8.6 during the study period. These conditions reflected the typical seasonal hydrographic variability of Vembanad Lake, with lower salinity during the monsoon due to freshwater inflow and higher salinity during the premonsoon period. All sampled fish originated from the same cage culture system, ensuring that reproductive observations were made under comparable environmental conditions.

2.2 | Data Recording and Image Processing

The excess moisture across the body was dried via tissue paper before recording body weight with a digital balance (Ishtaa 0.01 g sensitivity) and measuring total length using Vernier callipers (accuracy 0.02 mm). A longitudinal abdominal incision was made to dissect and collect the gonads for macroscopic observation following the criteria proposed in Ref. [23]. After removing blood and debris, the gonads were photographed on white paper and weighed. Ovaries were preserved in 10% neutral buffered formalin for histological analysis and oocyte size frequency assessment following the criteria proposed in Ref. [23].

2.3 | Histological Examination of the Gonads

Reproductive activity was assessed using macroscopic gonadal examination, histological analysis of ovarian tissue and oocyte size frequency distribution. The spawning season of *E. suratensis* was determined based on the occurrence of spawning-capable females, indicated by the most advanced oocyte development stage (Vtg3) in the ovaries, following the criteria proposed in Ref. [24]. From the 202 collected ovaries, a representative subsample of 54 ovaries representing various ovarian reproductive phases and fish sizes ranging in total length from 90 mm to 260 mm was selected for histological observation. The left lobe of each ovary was fixed in 10% neutral buffered formalin for histology, while the right lobe was preserved separately for whole-mount analysis to assess the oocyte size frequency distribution corresponding to each histological sample using the protocol outlined in Ref. [24]. Three cross sections from the anterior, middle and posterior regions of the left ovary were taken, each including the ovarian wall. Duplicate histological slides were prepared per ovary, with three sections per slide.

The ovaries were sectioned transversely, and histological slides were prepared via the paraffin embedding technique following the standard protocol described in Ref. [23]. Tissues were dehydrated in a graded ethanol series, cleared in xylene and embedded in paraffin at 60°C, with multiple paraffin baths to ensure complete impregnation. Sections of (5 μm thickness) were cut using a rotary microtome (Leica RM2125 RTS: Leica Biosystems), stained with haematoxylin–eosin, dehydrated, cleared and mounted in DPX. The slides were examined under a Leica DM6 binocular microscope, and images were captured using Leica Application Suite X (LAS X) software at various magnifications.

The histological slides were further examined to classify the ovaries into distinct reproductive phases following [20]. Oocyte development stages were identified following the classifications proposed by [5, 20, 25, 26], whereas early growth stages were defined according to Ref. [27]. The female reproductive phases were assigned based on the most advanced oocyte development stages (i.e., leading cohort of oocyte stages) present in the ovarian tissue.

In spawning-capable females, the occurrence of atresia was evaluated using histological criteria outlined in Ref. [28]. Atresia was quantified by examining 100–200 oocytes per ovary and recording the proportion of previtellogenic and vitellogenic oocytes undergoing degeneration, following the criteria outlined in Ref. [29]. Additionally, atretic oocytes were classified into α- and β-types, each with early and late stages, based on the morphological features such as zona radiata fragmentation, yolk granule disintegration and the presence of intracellular vacuoles, following Ref. [24].

2.4 | Measurement of Oocyte Diameter

The whole-mount ovarian subsamples corresponding to the histological sections were used to analyse the oocyte size frequency distribution. Each sample was weighed (i.e., 0.02–0.03 g to the nearest 0.001 g), and excess formalin was removed by blotting. Oocytes were separated from the connective tissue using fine paintbrushes, stained with rose bengal and placed in a petri dish for analysis following the procedure outlined in Ref. [30]. A photograph was taken via a stereomicroscope (Motic-SMZ168) connected to a camera with Image Plus 2.0 ML software. The diameter of the oocytes was measured from the captured images as the average of the longest axis (length of the longest dimension) and the shortest axis (width perpendicular to the longest axis) of individual oocytes by adjusting the magnification based on size. The diameters were then grouped into 100-μm size classes to assess the oocyte size frequency distribution following the protocol proposed in Refs. [30, 31].

2.5 | Seasonal Variation in the Oocyte Diameter of Advanced Vitellogenic Oocytes

The peak reproductive seasons were assumed from previous studies carried out in the study area, with the southwest monsoon (May–August) and the northeast monsoon (November–January) recognized as spawning periods [14]. For analyses, three seasons were defined: premonsoon (January–April), monsoon (May–September) and postmonsoon (October–December). To evaluate seasonal oocyte development, the average diameter of the 50 largest vitellogenic oocytes was measured monthly following Ref. [24].

2.6 | Variation in Oocyte Development Stages of Spawning-Capable Ovaries during the Spawning Season

The presence of different oocyte development stages in spawning-capable ovaries (Vtg3 as the leading cohort of oocytes) during the spawning season was determined following the criteria outlined in Ref. [24]. The oocyte diameter ranges for each

developmental stage were calculated from histological sections and applied to the whole-mount frequency distributions. The relative proportion of oocyte developmental stages was determined based on the occurrence of the most advanced stage and the proportional distribution of all stages within the ovary following Ref. [24]. The five digital microphotographs were captured from histological slides for each specimen, and all the oocytes within each microphotograph were identified and counted by oocyte developmental stages. The proportion of each oocyte development stage was expressed as a percentage of the total oocytes per image, and the mean stage composition was calculated from the five images per specimen following the criteria outlined in Ref. [32].

For each oocyte development stage, the diameters of 30 oocytes were measured by calculating the average of the major and minor axes. The upper and lower boundaries for each stage were determined using a 99% confidence interval. As these intervals did not overlap, the midpoint between adjacent confidence limits (i.e., average of the upper limit and lower limit of two adjacent oocyte stages) was used to define the threshold limits separating each oocyte development stage following the criteria outlined in Ref. [24]. The same protocol was applied to estimate the percentage of cortical alveolar (CA) oocytes and total vitellogenic oocytes (Vtg1, Vtg2 and Vtg3) for each ovarian reproductive phase.

2.7 | Characterization of the Oocyte Cohort in Spawning-Capable Ovaries of Female Pearlspot

A Gaussian mixture model (GMM) was applied to identify the oocyte cluster (components) on the basis of oocyte diameter in spawning-capable ovaries of pearlspot. A subsample of six fish ($n = 6$) with spawning-capable ovaries (Vtg3) was selected. From each ovary, a 0.02 sample was weighed (PO), and all the oocytes in that portion were measured to determine the size frequency distribution. These subsample data were then scaled to estimate the total number of oocytes in the whole ovary of each fish via the ratio of preserved total ovary weight (PW) to the weight of the subsample of preserved ovary (PW/PO) as the procedure outlined in Ref. [33]. The data from all the fish were then pooled into a single large distribution containing an estimated 12,546 oocytes. The GMM was applied to the full distribution of oocyte diameter data using the expectation maximization algorithm [34]. The likelihood function is defined as

$$L(\pi, \mu, \sigma|y) = \prod_{\{i=1\}}^{\{n\}} \sum_{\{k=1\}}^{\{K\}} \pi k f(yi|\mu k, \sigma k), \quad (1)$$

where, $y = y_1$ .....,y_n is the vector of oocyte diameters; $\pi = \pi_1$,.....π_n is the probability that an oocyte diameter comes from a particular component of the mixtures such that $o \leq \pi_k \leq 1$ and $\sum_{\{k=1\}}^{\{K\}} \pi_k = 1$, and f ($y_i$ |μ_k, σ_k) represents the probability of the observed data given the parameters specifying a Gaussian distribution for the K_{th} mixture component following Ref. [35].

2.8 | Estimation of the Size at Which Oocytes Are Recruited for Vitellogenesis in Spawning-Capable Ovaries

Logistic regression models were applied to estimate the probability of oocytes being recruited for vitellogenesis (ORS) following the methodology outlined in Ref. [30]. The model was fitted via a bias-reduction generalized linear model (GLM) with a binomial distribution and a logit link function. The oocyte development stage was coded as a binary response variable: 0 (previtellogenic oocytes) and 1 (vitellogenic oocytes). The logistic regression model was as follows:

$$P\left(Y = \frac{1}{OD}\right) = \frac{1}{1 + e\beta 0 + \beta 1 * OD}, \quad (2)$$

where P($Y = 1$|OD) represents the probability of an oocyte being recruited to vitellogenesis at oocyte size (OD), β_0 is the intercept and β_1 is the slope. The size at which 50% of the oocytes are likely to be recruited for vitellogenesis was estimated by dividing the intercept (β_0) by the slope (β_1). A bootstrap method with 999 iterations was used to estimate a 95% confidence interval around the oocyte recruitment size.

2.9 | Statistical Analyses

The Shapiro–Wilk test and Levene's test were applied to examine the normality of the data distribution, which was supported by a Q–Q plot for visual confirmation. The homogeneity of variance was verified via Levene's test. If these assumptions were violated, the Kruskal–Wallis test was employed for comparing multiple groups, followed by Dunn's post hoc test with Bonferroni adjustment for pairwise comparisons and the Wilcoxon rank sum test for comparing two groups with smaller sample sizes. To examine the uniformity of oocyte distribution within the ovaries, two-way ANOVA was conducted at the 5% significance level, considering both the ovarian lobes (left and right) and the sections of each lobe (anterior, middle and posterior). Additionally, exponential regression analysis was performed to explore the relationships between oocyte developmental stages and their corresponding diameters. A 99% confidence interval was calculated by multiplying the standard error by 2.56 or using the corresponding value. All the statistical analyses were conducted in RStudio software via the packages 'ggplot2' (for graphics), 'mclust' (for the GMM) and base R functions (for ANOVA, the Kruskal–Wallis rank sum test, the Wilcoxon rank sum test and regression analysis) [36].

3 | Results

3.1 | Oocyte Development Stages and Ovarian Reproductive Phases in *E. suratensis*

The histological examination of section *E. suratensis* ovaries revealed seven distinct oocyte developmental stages: the chromatin nucleolar (CN) and perinucleolar (PN) stages, in which oocytes are in the primary growth (PG) or previtellogenesis stage; the CA stage, which marks the onset of maturation; the primary, secondary and tertiary vitellogenesis stages (Vtg1–Vtg3, respectively), which represent progressive vitellogenesis; and the germinal vesicle migration (GVM), which indicates final oocyte maturation (FOM). Moreover, a postovulatory follicle (POF) was also observed, indicating signs of postspawning. Additionally, the early and late stages of both α- and β-atresia were also observed, indicating the completion of the spawning period (Figures 1 and 2). The oocyte diameter ranged from an average of 50.55 μm at the CN stage to 1452.80 μm at the GVM stage. A summary of the characteristics of each oocyte developmental stage is presented in Table 1 and Figure 1

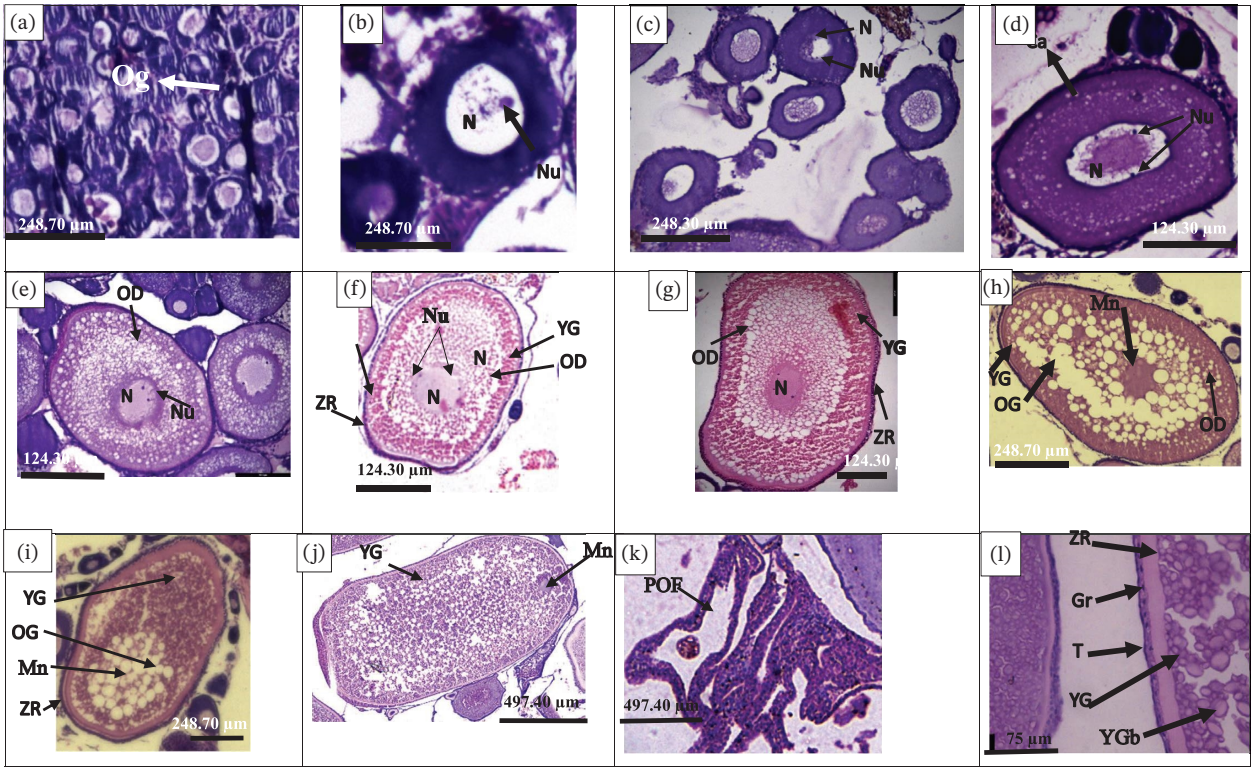

FIGURE 1 | Photomicrographs of histological sections of oocyte development stages in pearlspot. Primary growth of oocytes: (a) oogonia cell, 10x; (b) chromatin nucleolar stage, 10x; (c) perinuclear stage, 10x; (d) cortical alveolar stage, 20x; progression of the vitellogenesis stage (e–g): (e) primary vitellogenesis (Vtg1), 10x; (f) secondary vitellogenesis (Vtg2), 10x; (g) tertiary vitellogenesis (Vtg3), 20x; progression of oocyte maturation (h–j): (h) early germinal vesicle migration (GVM), 10x; (i) coalescence of oil droplets, 10x; (j) late germinal vesicle migration (LGVM), 5x; (k) postovulatory follicle complex (POFs), 5x; (l) follicle layer, 40x; Og = oogonial cell; CA = cortical alveolar; OD = oil droplet; OG = oil globule YG = yolk granule; YGb = yolk globule; Mn = migratory nucleus; N = nucleus; Nu = nucleolus; POF = postovulatory complex; ZR = zona radiata; Gr = granulosa cell; T = thecal layer. Scale: a, b, c, e, h, i: 248.70 µm; d, e, f, g: 124.30 µm; j, k: 497.40 µm; l: 75 µm.

The microscopic criteria used to categorize the ovarian reproductive phases of *E. suratensis* are presented in Figure 3.

The microscopic criteria used to categorize the ovarian reproductive phases of pearlspot are presented in Figure 3. The immature phase is gonadotropin independent and is characterized by the proliferation of oogonia and the occurrence of PG oocytes. As ovarian development progresses, the fish enters the development phase, which is a gonadotropin-dependent phase and marks the onset of sexual maturity. This phase has been characterized as the spawning preparation stage, which is characterized by rapid vitellogenesis and the presence of CA, Vtg1 and Vtg2 oocytes but lacks the most advanced vitellogenic (Vtg3) oocytes. The developing phase is followed by the spawning-capable phase, which is represented by the presence of the most advanced oocyte stages (Vtg3) along with the earlier vitellogenic oocytes. At this point, oocytes begin to receive hormonal signals for FOM, and the fish become capable of spawning within the current reproductive cycle. Batch fecundity is typically assessed during this phase in batch-spawning species. Within the spawning-capable phase, an actively spawning subphase is identified by the presence of oocytes at the migratory nucleus stage, indicating readiness for ovulation if appropriate environmental or physiological cues are received. The regressing phase marks the end of the reproductive cycle, distinguished by widespread atresia, the presence of POFs and a small number of residual healthy Vtg2 or Vtg3 oocytes. The phase is relatively short and is followed by the regenerating phase, during which the fish is sexually mature but reproductively inactive. During this phase, oocytes are gonadotropin independent, with oogonia undergoing mitotic proliferation and PG oocytes being predominant.

3.2 | Ovarian Organization

3.2.1 | Progression of Oocyte Developmental Stages and the Corresponding Oocyte Size Frequency Distribution Across Ovarian Reproductive Phases

The mean diameter of the most advanced oocyte stage (i.e., leading cohort) was measured for each ovarian reproductive phase. Oocyte diameter increased progressively with development, with significant differences among stages (Kruskal–Wallis rank sum test: $\chi^2 = 396.30$, $df = 5$, $p < 0.05$; Figure 4(a)). The pairwise comparison via the Dunn test with Bonferroni correction revealed no significant difference among PG-CA ($p > 0.05$), Vtg3-GVM ($p > 0.05$) and Vtg2-Vtg3 ($p > 0.05$) (Figure 4(a)). The oocyte size frequency distribution across reproductive phases is shown in Figure 4(b). The oocyte size distribution in the pearlspot exhibited continuous growth, with no distinct gap between the PG stage and the onset of vitellogenesis at 266.64 μm.

In the spawning-capable ovaries, a heterogeneous mixture of oocytes without a dominant cohort indicates asynchronous

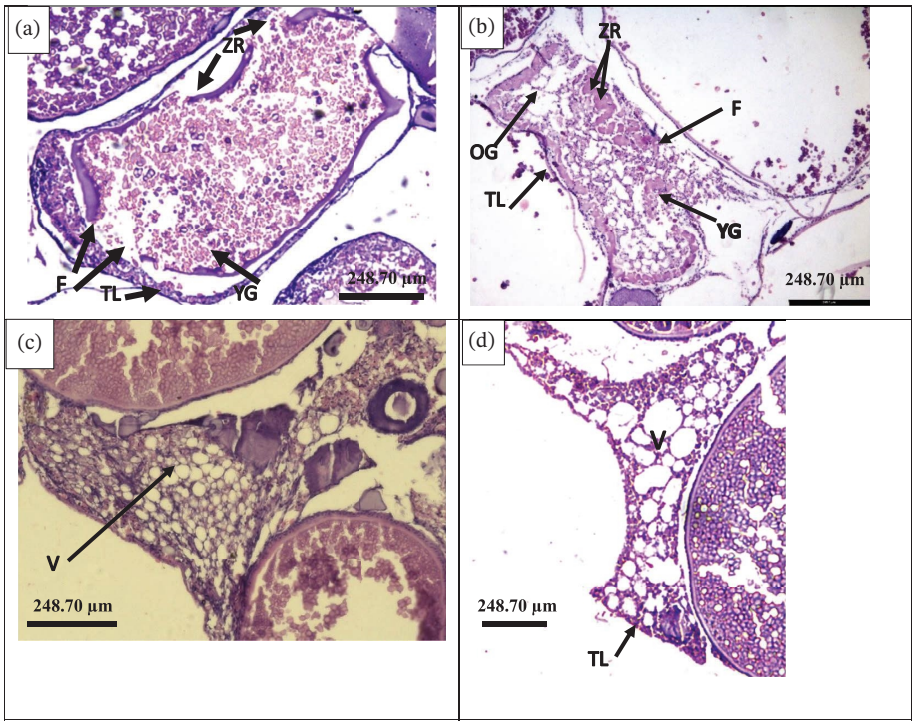

FIGURE 2 | Photomicrographs of ovarian histological sections illustrating various stages of atresia in pearlspot. (a) Early alpha atresia, 10x; (b) late alpha atresia, 10x; (c) early beta-atresia, 10x; (d) late beta-atresia, 10x; ZR = zona radiata, F = areas showing breakdown or disintegration of the zona radiata, TL = theca layer, YG = yolk granules, OG = oil globules, OD = oil droplets, and V = vacuoles. Scale: a, b, c, d: 248.70 µm.

oocyte development. In the immature phase, the PG oocytes included CN (40–80 μm) and perinucleolar (80–130 μm) stages, with a narrow size distribution. In the early development phase, the CA stage (130–210 μm) appears along with the PG oocyte, resulting in a right-skewed size distribution. The first transition of oocytes from the early developing phase (CA) to the vitellogenesis phase begins at a diameter of 266.64 μm (Figure 4(a)). As vitellogenesis progresses, oocyte size increases from 181.66 µm in Vtg1 oocytes to a maximum of 1047.19 µm in Vtg3 oocytes. In the spawning-capable phase, where Vtg3 is the leading cohort, a group of oocytes within the secondary growth phase begins to separate from the standing stock of vitellogenic oocytes, which are visible in the 700–800 µm size range (Figure 4(b)). Moreover, in females at the actively spawning subphase (with GVM oocytes as the leading cohort), a noticeable hiatus (gap) in oocyte size distribution appears, separating the future spawning batch from the standing stock of advanced vitellogenic oocytes in the 950–1250 µm size range (Figure 4(b)). Additionally, this spawning batch continues to mature through GVM towards FOM, followed by hydration and subsequent ovulation (Figure 4(b)), whereas the remaining advanced vitellogenic oocytes were retained for future replenishment of oocytes.

An exponential regression model was used to describe the relationship between oocyte developmental stage and diameter, showing a significant increase in oocyte size as development progresses in spawning-capable ovaries (Figure 5). This pattern highlights substantial yolk accumulation, especially during the late stages of vitellogenesis, leading to a sharp increase in oocyte size. The baseline diameter (38.098 μm) reflects early stage oocytes, whereas the growth rate coefficient (0.505) indicates accelerated expansion during vitellogenesis. This high growth rate coefficient highlights a rapid increase in size, which is especially pronounced during the transition from early vitellogenic stages (Vtg1 and Vtg2) to the advanced stage (Vtg3).

The seasonal variation in the oocyte diameter indicated continuous oocyte recruitment and maturation in *E. suratensis* (Figure 6). During premonsoon, oocyte diameter moderately increased ($R^2 = 0.27$) due to the active recruitment in vitellogenesis. In the monsoon season, diameter showed a decreasing trend ($R^2 = 0.44$), resulting from either the release of the spawning batch or the onset of atresia. The postmonsoon season showed a slight upward trend ($R^2 = 0.17$), indicating the initiation of a new reproductive cycle with the recruitment of a new cohort of oocytes in the vitellogenic phase. The mean oocyte diameter varied significantly across seasons (Kruskal–Wallis rank sum test: $\chi^2 = 33.51$, df = 2, $p < 0.05$). The pairwise Dunn test with Bonferroni correction showed significant differences between monsoon and postmonsoon ($p < 0.05$) and between postmonsoon and premonsoon ($p < 0.05$), whereas no significant differences were observed between the monsoon and premonsoon ($p > 0.05$) (Figure 1). These results support asynchronous oocyte development, with overlapping phases of oocyte recruitment and degeneration throughout the year.

The stacked bar plot illustrates the relative proportion of oocyte developmental stages across ovarian reproductive phases in pearlspot (Figure 7). The presence of CA stages was perceptible across the ovarian reproductive phases and predominant in the developing phase (Vtg1 as the leading cohort), and declined progressively, reaching the lowest in the spawning-capable phase (GVM as the leading cohort). As ovarian development proceeds through the Vtg2 and Vtg3 phases, the proportion of secondary and tertiary vitellogenic oocytes increases, while primary vitellogenic oocytes remain consistent. In the spawning-capable

TABLE 1 | Microscopic characterization of oocyte developmental stages in pearlspot, adopted from Costa (2015).

Oocyte development stages	Histological descriptions	99% CI	Range
Previtellogenic growth			
Chromatin nucleolar (CN) stage	Oocytes are compact, angular and unyolked with a dark purple cytoplasm and characterized by the presence of at least one conspicuous central large nucleolus ($55.62 \pm 10.68\ \mu$m, $n = 150$)	51.77–59.48	40–80
Perinucleolar stage (PN)	Large and rounder than CN, unyolked oocytes with cytoplasm staining light purple and nucleus showing several nucleoli positioned along the inner edge of the nuclear membrane. The formation of the follicular layer surrounding the oocyte indicates the initiation of chorion cells. ($104.62 \pm 13.46\ \mu$m, $n = 160$)	98.59–110.66	80–130
Cortical alveolar (CA)	CA marks the onset of secondary growth with small oil droplets, and cortical alveoli begin to appear along the cytoplasm periphery. The nucleoli remain perinucleolar, and the nuclear membrane begins to fold. A thin acidophilic zona radiata first became visible, while the yolk granules were still absent ($160.48 \pm 19.80\ \mu$m, $n = 130$)	143.04–173.62	130–210
Vitellogenic oocyte growth			
Primary vitellogenesis (Vtg1)	Eosinophilic yolk granules start to appear as a ring at the cytoplasm periphery, while oil droplets occupy a larger portion of the cytoplasm, and cortical alveoli are aligned at the periphery of the oocytes ($266.64 \pm 57.37\ \mu$m, $n = 120$)	246.70–286.56	210–400
Secondary vitellogenesis (Vtg2)	The relative proportion of yolk granules to oil droplets increases, with both occupying a similar cytoplasmic area, and the oil droplets arranged around the nucleus ($492.73 \pm 48.15\ \mu$m, $n = 90$)	474.44–511.026	400–620
Tertiary vitellogenesis (Vtg3)	The relative proportion of yolk granules to oil droplets increases, while oil droplets enlarge and occupy less cytoplasmic area as compared to yolk granules and are concentrated around the nucleus ($779.37 \pm 101.55\ \mu$m, $n = 100$)	740.18–818.56	620–875
Oocyte maturation			
Germinal vesicle migration (GVM)	The main characteristics of this stage are the eccentric position of the nucleus (germinal vesicle). As the oocyte enters the final maturation phase, the nucleus migrates towards the animal pole and the oil droplets coalesce to form larger oil globules, which become apparent at this stage ($1040.75 \pm 214.14\ \mu$m, $n = 64$)	956.59–1138.65	875–1450
Atresia			
Early-α atresia	The yolk granules and oil droplets are prominent within the oocyte; however, the rupture of the zona radiata and nuclear breakdown are evident		
Late α atresia	Extensive fragmentation of zona radiata (ZR) is observed, extending into the cytoplasm along with the nucleus disintegration. Yolk granules are fused, and oil droplets have merged into larger oil globules.		

(Continues)

TABLE 1 | (Continued)

Oocyte development stages	Histological descriptions	99% CI	Range
Early β atresia	Complete resorption of yolk granules and nucleus is observed with only a few fragments of ZR. Granulosa cells are found within the follicle, and a large number of vacuoles start to form		
Late β atresia	The cells become small and irregular, with few or no granulosa cells remaining inside. The ZR is completely resorbed, and vacuoles are enlarged and more abundant than in the previous stage		

Note: The oocyte diameters were measured from histological sections with the mean diameter ± standard deviation, and the total number of oocytes measured (*n*) for each developmental stage is given in parentheses. CI: 99% lower and 99% upper confidence intervals.

phase (GVM as the leading cohort), mature oocytes co-occur with substantial proportions of Vtg1 and Vtg2, whereas Vtg3 oocytes noticeably decline, indicating their progression towards final maturation.

The monthly distributions of oocyte stages in spawning-capable ovaries of pearlspot are shown in Figure 8. The proportion of CA oocytes relative to total vitellogenic oocytes remained consistent across the months, with a mean of 40.85 ± 2.47, ranging from a minimum of 37.67% in July to a maximum of 45% in April, with no significant seasonal variation (Kruskal–Wallis rank sum test: $\chi^2 = 10.32$, df = 7, $p > 0.05$). The overall proportion of total vitellogenic oocytes increased slightly during the spawning season from 50.60% in May to 58.33% in July; however, this change was not statistically significant across months (Kruskal–Wallis rank sum test: $\chi^2 = 9.12$, df = 7, $p > 0.05$). CA and Vtg1 oocytes were the dominant oocyte stages across all months, whereas Vtg2 and Vtg3 oocytes were present in smaller proportions. Notably, a slight increase in the proportion of Vtg3 was observed during May and July, corresponding to peak reproductive activity, and the proportion of Vtg3 subsequently declined in the postspawning months. The relative proportion of atretic oocytes increased towards the end of the reproductive season, rising from 11.20% in August to 12.30% in December. There was a significant difference in the percentage of atretic oocytes across months (Kruskal–Wallis rank sum test: $\chi^2 = 22.46$, df = 7, $p < 0.05$). The observed pattern indicates that oocytes not released during the spawning season were progressively reabsorbed through atresia during the postspawning period. The seasonal increase in atresia indicates a regulatory mechanism for eliminating surplus oocytes and reallocating energy following intensive spawning activity, which is characteristic of asynchronous, indeterminate spawners.

The difference in the percentage of oocyte stages between fish that had spawned and those showing no signs of spawning is illustrated in Figure 9. Notably, the proportion of total vitellogenic oocytes (Vtg1, Vtg2 and Vtg3) over the total pool of oocytes was higher in nonspawned fish (58 ± 4.56%) than in spawned fish (47 ± 3.56%). However, this difference was not statistically significant (Wilcoxon rank sum test: $W = 27.98$, $p > 0.057$, *effect size = 0.82*). Additionally, when only advanced vitellogenic oocytes (Vtg3) were considered, their mean proportion was lower in spawned fish (8 ± 2.96%) than in nonspawned fish (12 ± 3.21%). This difference was also not statistically significant (Wilcoxon rank sum test: $W = 30.95$, $p > 0.05$*; effect size: 0.82*).

The oocyte size frequency distribution revealed continuous oocyte growth without a gap between previtellogenic and vitellogenic oocytes for each ovarian reproductive phase across the sampled month (Figure 10).

The smoothed frequency plot exhibited multiple distinct peaks, representing different oocyte developmental stages in pearlspot (Figure 11). The narrow peaks at 30–60 μm, 70–100 μm and 110–160 μm corresponded to the CN stage, PN and CA stages, indicating uniform oocyte sizes. Slightly broader curves at 200–350 μm and 450–550 μm in the primary and secondary vitellogenic stages (Vtg1 and Vtg2) reflected a moderate size variation, while the tertiary vitellogenic stage (Vtg3) showed a broader peak at 650–800 μm, indicating greater variability in the oocyte diameter. The oocyte size distribution in spawning-capable ovaries

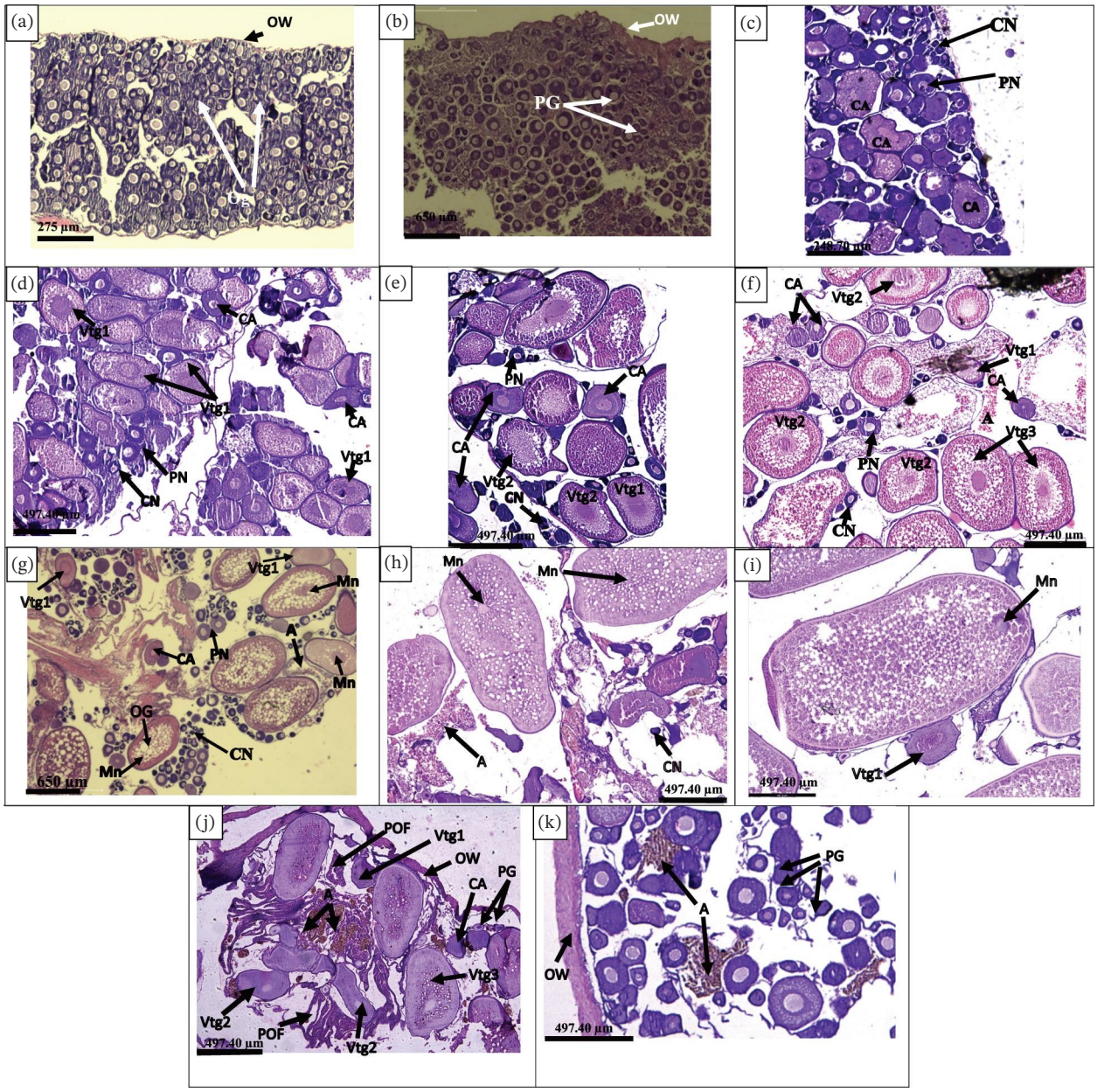

FIGURE 3 | Photomicrographs of histological sections of different ovarian reproductive phases in pearlspot: (a) proliferation of oogonia (Og = oogonial cell), 10x; (b) immature phase (PG=primary growth, CN=chromatin nucleolar, PN=perinucleolar), 5x; (c) early development phase (CN=chromatin nucleolar, PN = perinucleolar, CA = cortical alveolar stage), 10x; (d-e) developing phase (Vtg1 primary vitellogenesis, Vtg2 = secondary vitellogenesis as a leading cohort of oocytes), 5x; (f) spawning-capable phase (Vtg3 tertiary vitellogenesis), 5x; (g–i) actively spawning subphase (GVM = germinal vesicle migration) in the early and late stages of nuclear migration, 5x; (j) actively spawning subphase with postovulatory follicles (POFs), 5x; (k) regenerating phase, 5x; OW = ovarian wall; N = nucleus; Mn = migratory nucleus; OG = oil globule; A = atresia. Scale: a: 275 µm; b, g: 650 µm; c: 248.70 µm; d, e, f, h, i, j, k: 497.40 µm.

showed a continuous growth pattern without a distinct gap between previtellogenic and vitellogenic oocytes. The analysis revealed that the advanced vitellogenic oocytes (Vtg3) develop from Vtg2, which gradually increase in the diameter to form a future spawning batch. The variability observed in oocyte size distribution in the vitellogenic stages is likely due to the ongoing process of oocyte recruitment.

The probability of the oocyte size at which 50% of the oocytes are recruited for vitellogenesis was determined via a sigmoid relationship in three different ovarian phases of spawning-capable ovaries in pearlspot (Table 2; Figure 12). The size at which 50% of the oocytes are recruited for vitellogenesis was estimated to be 240.45 µm in spawning-capable ovaries (Vtg3), 210.88 µm in spawning-capable ovaries (GVM) and 195.98 µm in spawning-capable ovaries (POF). Oocytes below these threshold levels are predominantly in the previtellogenic phase, whereas above it, they transition into vitellogenesis and maturation.

3.3 | Characterization of the Oocyte Cohort in Spawning-Capable Ovaries Of Female Pearlspot

In general, GMMs represent an unsupervised machine learning technique that can be used to explain clustered data. The model

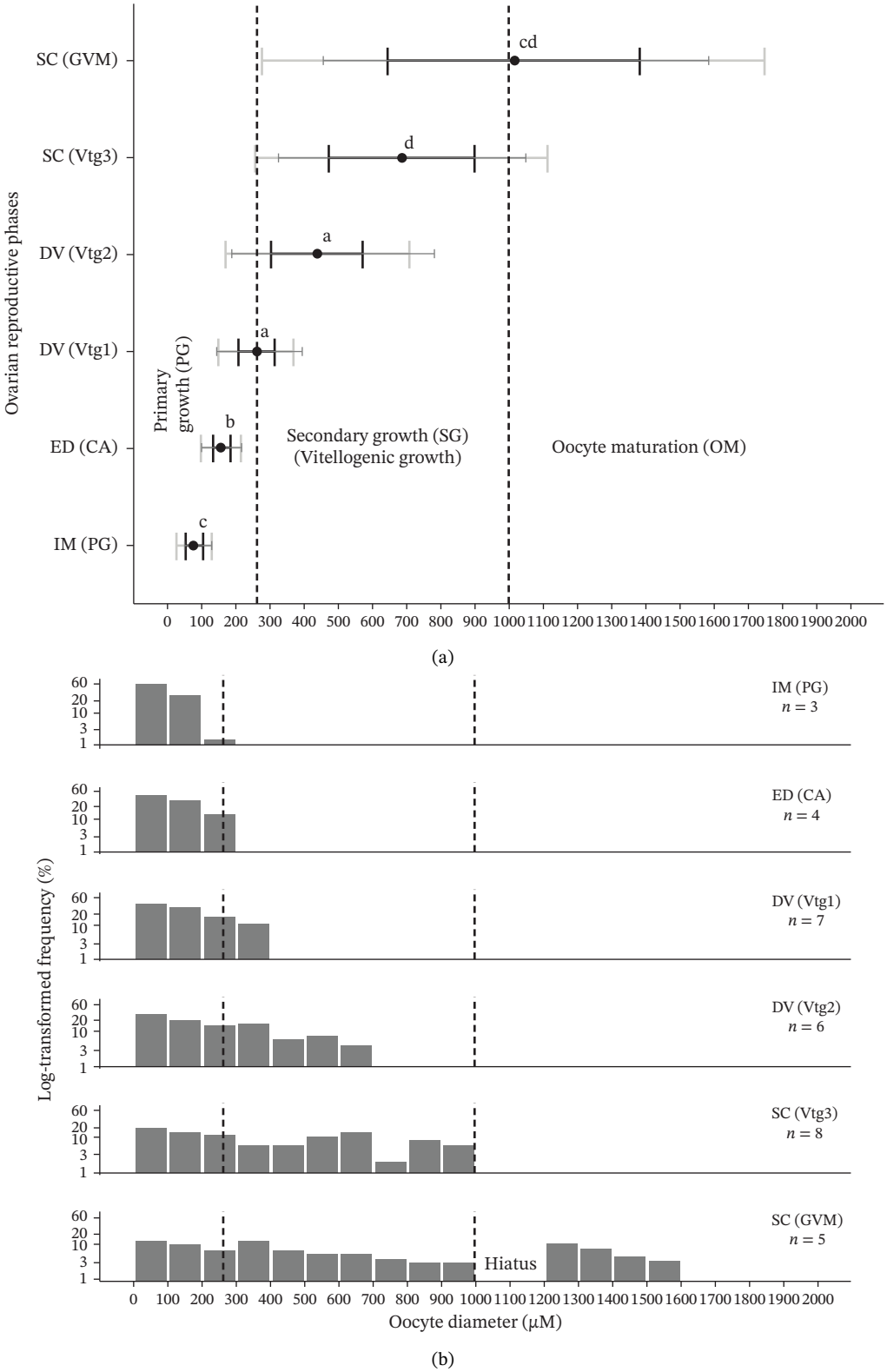

FIGURE 4 | Illustration of ovarian organization in pearlspot with (a) progression of the leading cohort of oocyte developmental stages in subsamples representing each ovarian reproductive phase. Oocyte diameter was measured from histological sections of 30 oocytes representing the leading cohort in each ovarian reproductive phase. The black circles indicate the mean oocyte diameters, the wide black and grey bars represent one and two standard deviations, respectively, and the narrow grey bars indicate the full range (minimum to maximum). Different letters denote statistically significant differences ($p < 0.05$) among oocyte developmental stages. The vertical dashed line separates the oocyte growth stages at the midpoint between the mean oocyte diameters of adjacent developmental stages, and (b) the log-transformed oocyte size frequency distribution across reproductive phases. n = number of individuals in each ovarian reproductive phase used for estimating oocyte size frequency distribution. Notes: IM(PG): immature phase with PG oocytes as a leading cohort; ED(CA): early development phase with CA oocytes as a leading cohort; DV(Vtg1): developing phase with primary vitellogenic oocytes; DV(Vtg2): Developing phase with secondary vitellogenic oocytes; SpCa (Vtg3): spawning-capable phase with tertiary vitellogenic oocytes; SpCa (GVM): spawning capable phase with GVM oocytes. To enhance visualization, the oocyte size distribution was natural log (ln) transformed and summed into 100-μm-diameter intervals.

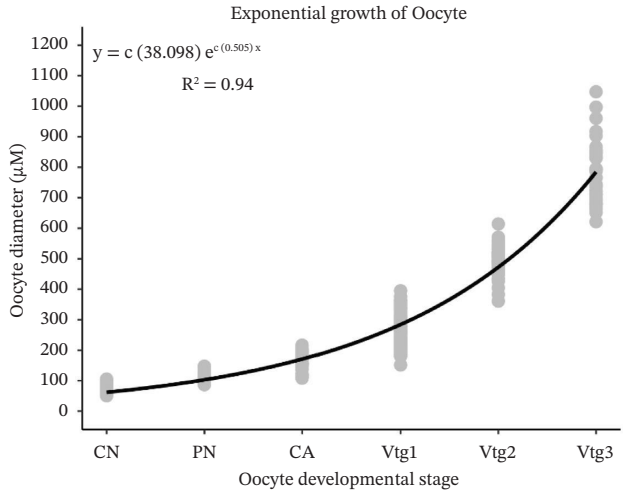

FIGURE 5 | Relationship between oocyte diameter and oocyte developmental stages in spawning-capable ovaries (Vtg3 oocytes as the leading cohort) of pearlspot, including chromatin nucleolar (CN), perinucleolar (PN), cortical alveolar (CA) and vitellogenic stages: primary (Vtg1), secondary (Vtg2) and tertiary (Vtg3).

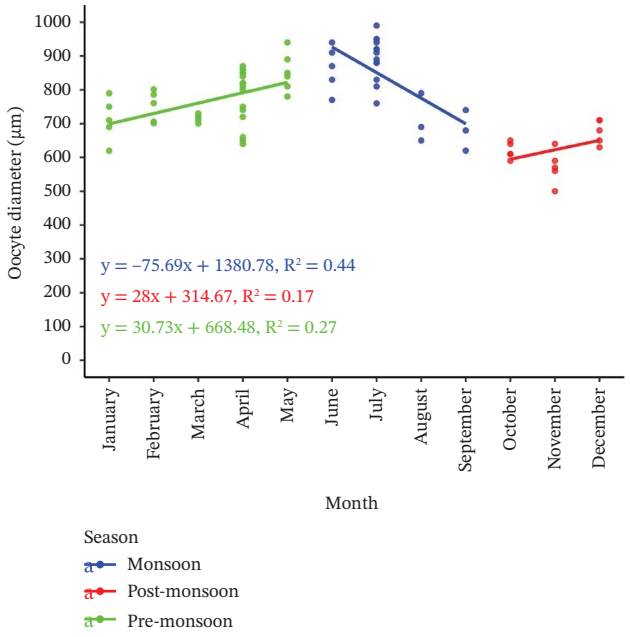

FIGURE 6 | Comparison of the seasonal trends in oocyte diameter in pearlspot. The regression line illustrates the direction and strength of the variation in oocyte size across seasons.

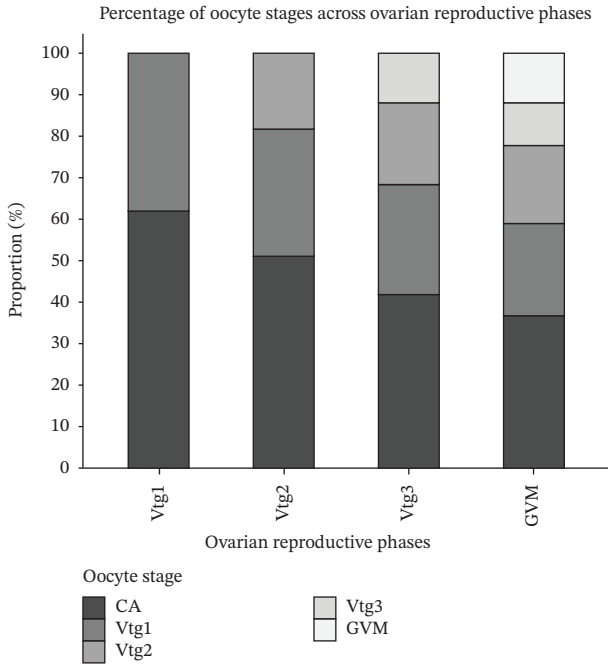

FIGURE 7 | The percentages of oocyte development stages across ovarian reproductive phases were classified as the developing phase (Vtg1 and Vtg2 as the leading cohort of oocytes) and the spawning-capable phase (Vtg3 and GVM as the leading cohort of oocytes). Sample sizes for each stage were Vtg1 ($n = 6$), Vtg2 ($n = 5$), Vtg3 ($n = 7$) and GVM ($n = 4$).

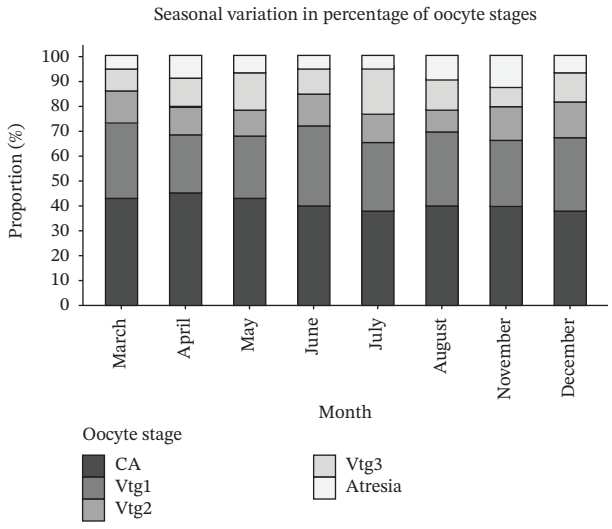

FIGURE 8 | Seasonal changes in the percentage of oocyte stages in spawning-capable females (Vtg3 as the leading cohort) were recorded from March to December. The stacked bar plot shows the mean proportion (%) of each oocyte stage across the sampling month. Two individuals were analysed per month.

identified five statistically distinct clusters based on the lowest Bayesian information criterion (BIC), which provides the best fit to the model corresponding to the development stages from PG through Vtg3/OM (Table 3; Figure 13). Each cluster identifies its own mean, variance and proportion of oocyte size distribution.

The first component (blue curve) shows high-density peaks at smaller diameters, indicating a large population of PG oocytes, i.e., the CN and PN stages. The second component (red curve) corresponds to the early development phase, i.e., the CA stage. The third component (green) represents intermediate-sized oocytes corresponding to the primary vitellogenic oocytes. The fourth and fifth components (orange and purple) correspond to larger oocytes, likely corresponding to secondary and tertiary vitellogenesis oocytes. The fifth component signifies a smaller proportion of oocytes that progress towards the advanced vitellogenesis stage (Vtg3). This stage is marked by a bold, dashed black vertical line with a mean oocyte diameter of 745.95 μm and a 95% confidence interval (CI) ranging from 620.84 to 875.43 μm.

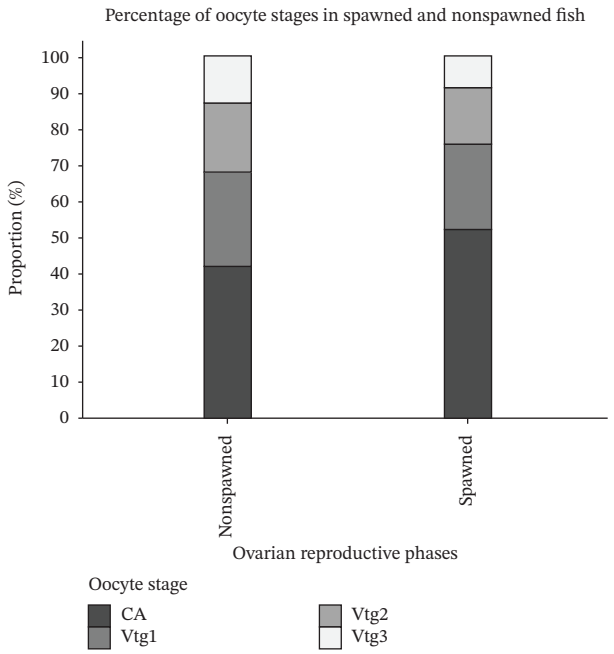

FIGURE 9 | Differences in the percentage of oocyte stages between spawned fish (POFs) and nonspawned fish. The stacked bar plot shows the mean proportion (%) of each oocyte development stage across all the samples. Sample sizes were $n = 3$ for spawned fish and $n = 6$ for nonspawned fish.

4 | Discussion

A comprehensive assessment of ovarian development in a fish is important for understanding the oocyte maturation pattern, spawning strategy and oocyte recruitment pattern [37, 38]. In *E. suratensis*, distinct oocyte developmental stages were observed across ovarian reproductive phases, ranging from PG oocytes in immature ovaries to fully mature oocytes at the GVM in spawning-capable females. The progressive appearance of CA oocytes followed by successive vitellogenic stages (Vtg1–Vtg3) indicates continuous oocyte growth rather than synchronized cohort development. Similar oocyte development stages have been reported in asynchronous fish species by Wallace and Selman [39], West [25], and Murua and Saborido-Rey [5]. The simultaneous presence of multiple oocyte development stages and oocyte size classes within a single ovary, together with the absence of a clear gap between previtellogenic and vitellogenic oocytes, confirms an asynchronous ovarian organization. This pattern is characteristic of indeterminate spawners, in which oocytes are continuously recruited throughout the spawning season rather than being fixed before the spawning season [5, 14, 15, 22]. Similar asynchronous recruitment has been reported in several tropical species, including *Anchoa filifera, Cetengraulis edentulus, Citharichthys spilopterus, Stellifer brasiliensis, S. rastrifer* and *Menticirrhus americanus* [30]. The presence of POFs alongside advanced vitellogenic oocytes further supports a multiple batch-spawning strategy, indicating that new cohorts of oocytes are recruited soon after spawning events. This reproductive pattern allows pearlspot to sustain prolonged spawning activity under favourable environmental conditions, which is advantageous for broodstock management and seed production in cage culture systems.

Oocyte size frequency distribution is a key indicator for determining fecundity type in many fish species based on whether a clear gap exists between previtellogenic and vitellogenic oocyte cohorts [8, 24, 40]. In this study, no clear separation was observed between the primary and secondary oocyte growth stages in the size frequency distribution, and this continuous pattern was consistent across all ovarian reproductive phases and sampling months. Such continuity suggests that previtellogenic oocytes are continuously recruited into vitellogenesis throughout the spawning season. Similar patterns have been reported in indeterminate spawners such as Atlantic sardine (*Sardina pilchardus*) by Lowerre-Barbieri et al. [38], northern anchovy (*Engraulis mordax*) by Hunter and Macewicz [33], and *Katsuwonus pelamis* by Stequert and Ramcharrun [41], respectively. The presence of multiple overlapping vitellogenic cohorts further supports an asynchronous ovarian organization, where oocytes at different developmental stages coexist and mature at different rates [21, 42–44]. This recruitment pattern is characteristic of species with indeterminate fecundity, in which annual egg production is fixed during the spawning season but depends on continuous oocyte recruitment and repeated spawning [45]. In asynchronous spawners, previtellogenic oocytes are continuously recruited into the vitellogenic pool throughout the spawning season, allowing repeated batch-spawning and prolonged reproductive activity [46, 47]. This continuous recruitment prevents the formation of a distinct gap between early and late oocyte stages. In contrast, synchronous and group-synchronous species exhibit determinate fecundity, where oocyte recruitment ceases once vitellogenesis begins. Synchronous ovaries contain a single, uniformly developing cohort of oocytes, typically forming a bell-shaped size distribution, while group-synchronous ovaries show two clearly separated cohorts: a reserve pool of previtellogenic oocytes and a mature, synchronized vitellogenic group [5]. The absence of such cohort separation in pearlspot indicates an asynchronous ovarian organization and supports its classification as an indeterminate, multiple-batch spawner.

Fecundity in batch-spawning species is classified as either indeterminate or determinate based on the patterns of oocyte recruitment [22]. In indeterminate spawners, previtellogenic oocytes continue to be recruited into vitellogenesis throughout the spawning season, meaning that the total annual egg production is not fixed in advance. Instead, fecundity depends on the number of eggs released per spawning event, spawning frequency, and the duration of the spawning period based on [48]. In contrast, determinate spawners complete oocyte recruitment before the onset of spawning season, and no additional oocytes enter vitellogenesis once the reproductive season begins [5, 22]. In pearlspot, the continuous presence of multiple oocyte developmental stages and the absence of a distinct size gap between previtellogenic and vitellogenic oocytes provide strong histological evidence for ongoing oocyte recruitment. These findings, supported by oocyte size frequency distributions from whole-mount preparations, served as the primary criterion for indeterminate fecundity and indicate that pearlspot follows a multiple-batch-spawning strategy.

In the present study, the relative proportions of CA and vitellogenic oocytes remained stable across months in spawning-capable females, with no significant seasonal decline in

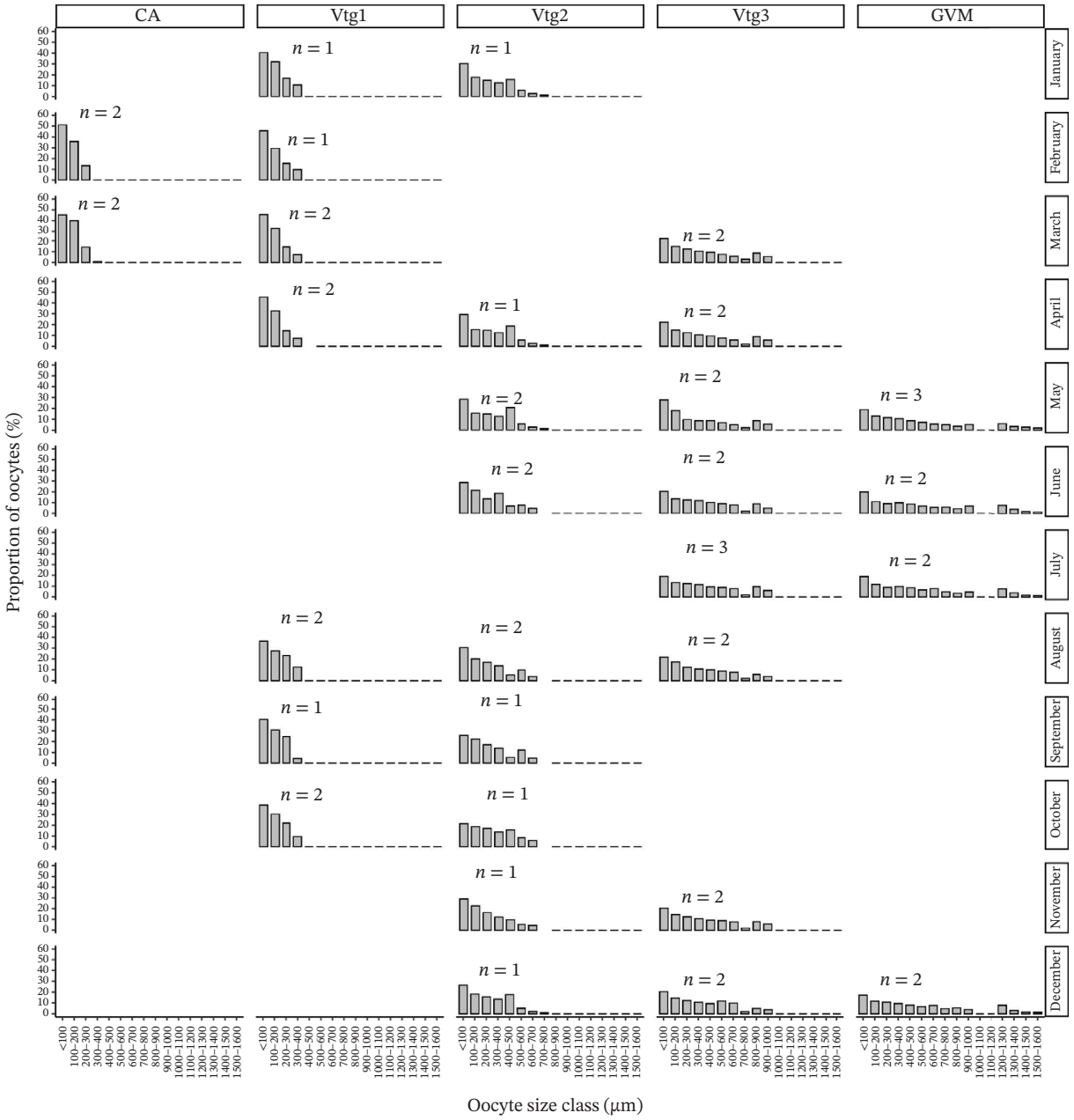

FIGURE 10 | Oocyte size distribution in each ovarian reproductive phase across sampling months. $n =$ indicates the number of samples in each ovarian reproductive phase. Oocyte diameters were grouped into size classes with 100-μm intervals.

vitellogenic oocytes. This pattern indicates continuous recruitment of previtellogenic oocytes into secondary growth throughout the spawning season. Such ongoing recruitment has been described as *de novo* vitellogenesis by Murua and Saborido-Rey. [6]. Similarly, Brown-Peterson et al. [49] reported that the persistent presence of CA and vitellogenic oocytes across the spawning period is a key feature of indeterminate spawners, as observed in Gulf menhaden (*Brevoortia patronus*). In contrast, determinate species exhibit a decline in previtellogenic and vitellogenic oocyte proportions during the spawning season, as these oocytes are not replenished once spawning begins. The consistent presence of both previtellogenic and vitellogenic stages observed in pearlspot provides a second line of evidence supporting its classification as an indeterminate, multiple-batch spawner. In the present study, the mean diameter of the most advanced vitellogenic oocytes (Vtg3) declined progressively as the spawning season advanced, indicating continuous recruitment of early vitellogenic oocytes into the vitellogenic pool. Similar seasonal reductions in advanced oocyte size have been reported for *Merluccius merluccius* (Murua and Motos [50]) and *Thunnus albacares* (Zudaire et al. [24]), a pattern typical of species with indeterminate fecundity. This reflects repeated spawning events, during which the largest oocytes are released and replaced by newly recruited cohorts, leading to a progressive reduction in mean oocyte diameter over the spawning season, as also reported by Hunter et al. [22]. In contrast, synchronous spawners typically exhibit increasing oocyte diameters through the spawning season, as a single cohort matures without further recruitment [50]. The observed seasonal decline in advanced oocyte size in pearlspot, therefore, provides a third line of

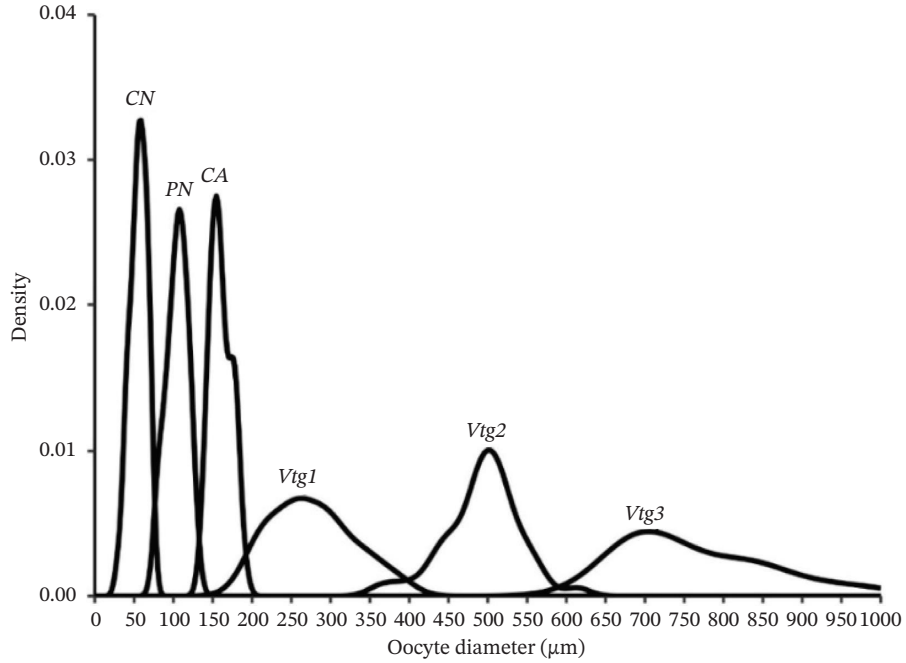

FIGURE 11 | Smoothed frequency plot showing oocyte diameter distribution in spawning-capable ovaries of pearlspot. The distinct peaks correspond to specific oocyte developmental stages: chromatin nucleolar (CN), perinucleolar (PN), cortical alveolar (CA) and vitellogenic stages (Vtg1, Vtg2 and Vtg3).

TABLE 2 | Estimation of the equation parameters and oocyte recruitment size by ovary phase.

Ovarian reproductive phases	*n*	Size at oocyte recruitment (μm)	β_0 (C.I.)	β_1 (CI)
Spawning capable ovaries (POFs)	120	195.98 (188.25–202.98)	−13.08 (−18.09–−9.46)	0.06 (0.05–0.09)
Spawning capable ovaries (GVM)	110	210.88 (203.42–217.34)	−11.56 (−15.51–−8.60)	0.05 (0.04–0.07)
Spawning capable ovaries (Vtg3)	220	240.45 (226.62–254.89)	−15.07 (-17.06–−0.27)	0.06 (0.04–0.09)

Note: β_0: intercept, β_1: slope, CI: 95% lower and 95% upper confidence intervals. 95% confidence interval of 50% of the total number of oocytes recruited for vitellogenesis given in brackets. n = total number of oocytes measured.

evidence supporting its classification as an indeterminate, multiple-batch spawner. In the present study, widespread resorption of vitellogenic oocytes was observed during August–September, coinciding with the decline of the peak reproductive activity, whereas atresia remained minimal during the active spawning season. This temporal pattern suggests that oocytes not released during repeated spawning events were subsequently eliminated through atresia [6, 28, 42, 43, 48]. The degeneration process in pearlspot followed the typical α- and β-atresia sequence described for *E. mordax* (Engraulidae) by Hunter and Macewicz [42], where α-atresia involves breakdown of the granulosa and theca layers, and β-atresia results in the complete resorption of yolk materials. Wallace and Selman [39] characterized atresia as a 'mopping-up' mechanism in fishes with asynchronous ovarian organization allowing the ovary to remove surplus oocytes after prolonged spawning activity. In contrast, determinate spawners generally exhibit a low level of atresia, as their annual fecundity is fixed before the spawning season. Atresia in teleost fishes is influenced by multiple factors, including temperature fluctuations, starvation and physiological stress [51]. Under favourable environmental and nutritional conditions, fish can sustain high spawning activity; however, when these conditions deteriorate, widespread atresia signals the termination of the reproductive season. Atresia represents an energy-regulating mechanism through which the ovary resorbs surplus oocytes to maintain physiological balance and redirect resources to somatic maintenance. This process allows indeterminate spawners to adjust their reproductive output according to prevailing environmental conditions. The consistent occurrence of postspawning atresia in pearlspot reflects this adaptive strategy, where excess oocytes produced during prolonged spawning are subsequently eliminated [24, 51]. Such dynamic regulation of oocyte numbers is a defining feature of indeterminate fecundity, providing the fourth criterion supporting the classification of pearlspot as an indeterminate, multiple-batch spawner.

In the present study, no significant difference was observed in the relative proportion of advanced vitellogenic oocytes (Vtg3) between spawned females (with signs of POFs) and nonspawned females. A similar pattern has been reported for *M merluccius* by Murua and Motos [50]. This likely reflects the continuous replenishment of advanced vitellogenic oocytes following spawning, a characteristic feature of indeterminate,

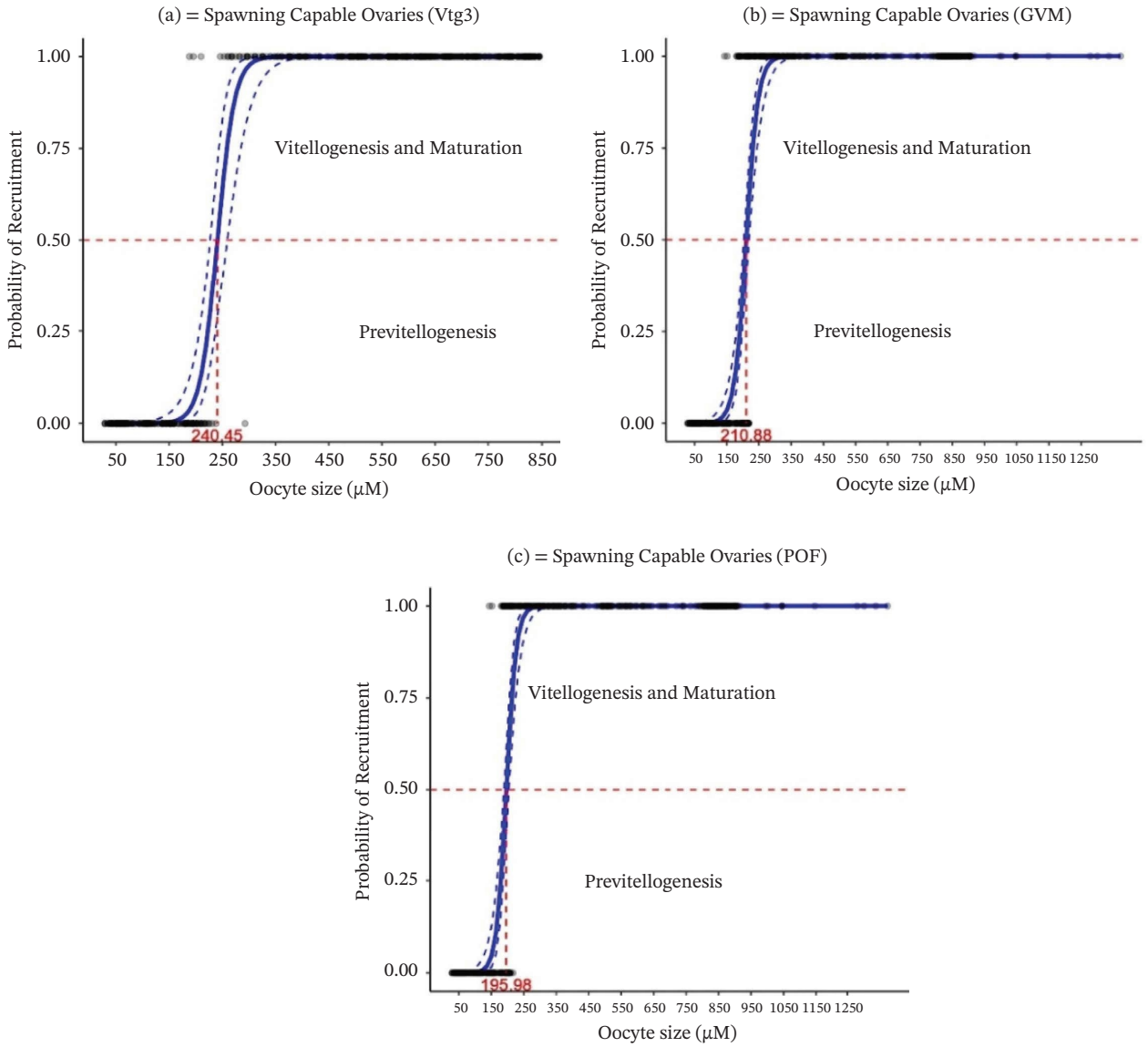

FIGURE 12 | Logistic regression model showing the probability of oocyte recruitment into vitellogenesis as a function of oocyte diameter (μm) in three phases of spawning-capable ovaries: (a) = spawning-capable ovaries (Vtg3), (b) = spawning-capable ovaries (GVM) and (c) = spawning-capable ovaries (POFs) of *E. suratensis*. Each black dot represents an individual oocyte classified as either vitellogenic (1) or previtellogenic (0). The solid blue curve shows the predicted probability of recruitment into vitellogenesis, whereas the blue dashed curves represent the 95% confidence intervals of the model estimate. The fitted values for the logit regression are based on a GLM and a nonparametric bootstrap method.

TABLE 3 | Gaussian mixture model (GMM) cluster statistics.

Cluster or components	Mean oocyte diameter (μm)	Variance	Proportion of oocyte (%)
1	55.87	10.98	28.74
2	134.32	27.50	27.35
3	278.67	56.05	16.74
4	497.02	39.65	15.38
5	745.95	70.50	11.76

Note: Estimated means, SDs, and proportions of oocytes for the five Gaussian curves.

batch-spawning species. The simultaneous presence of multiple oocyte development stages in spawned females indicates rapid recruitment of previtellogenic oocytes into the vitellogenic pool. Such rapid replenishment suggests a short interspawning interval, during which the ovary rapidly recruits new oocytes into advanced vitellogenic oocytes to support successive spawning events, as noted by Murua et al. [5].

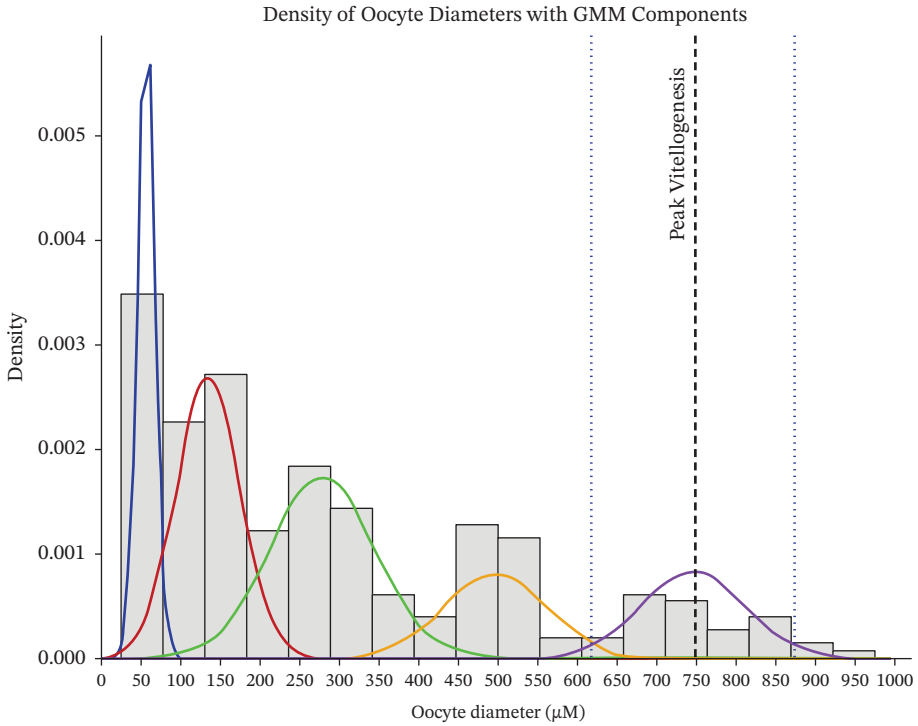

FIGURE 13 | The plot illustrates the density distribution of oocyte diameters in pearlspot, modelled via a Gaussian mixture model (GMM) with five components. The histogram (grey bars) represents the empirical distribution of oocyte sizes, scaled to density. Overlaid curves are fitted with five Gaussian finite mixture model curves, each representing a Gaussian component with a specific mean, standard deviation and relative proportion in the sample.

In the present study, multiple oocyte cohorts were observed throughout the spawning season without a dominant size class, indicating asynchronous ovarian development. A distinct gap in oocyte development occurred only at the GVM stage, separating the spawning batch (mature oocytes) from the pool of secondary vitellogenic oocytes and confirming a batch-spawning pattern. This gap became evident when the oocyte diameter reached 900–1000 μm. A similar separation between mature and vitellogenic oocytes in ripe ovaries was reported by West [25]. According to Heins and Brown-Peterson [52], a batch or clutch refers to a group of oocytes that develop synchronously and are spawned over a short period. Bindu [16] reported a slightly larger gap at 1500 μm in pearlspot from Vembanad Lake, which may reflect differences in environmental conditions, population genetics, sampling periods and measurement methods. These ovarian patterns reflect frequent clutch recruitment and short interspawning interval traits, typical of batch-spawning species with prolonged reproductive seasons in low-latitude regions [53, 54]. This observation aligns with the findings of Varghese [12], who reported that 46% of spawners exhibited multiple spawning events, with interspawning intervals ranging from 10 to 308 days under indoor conditions in fibre reinforced tanks. However, group-synchronous species also exhibit batch spawning despite having determinate fecundity. In such species, a single distinct cohort separates from the pre-vitellogenic pool and matures synchronously, as observed in Pacific halibut [55]. In contrast, in asynchronous species like pearlspot, the spawning batch (mature oocytes) separates from the advanced vitellogenic oocytes during maturation, enabling continuous oocyte recruitment.

The batch-spawning pattern observed in pearlspot may be attributed to its relatively high metabolic rate and the short oocyte growth period in relation to its extended spawning season. This is consistent with the findings of Hunter et al. [48], who reported a link between high metabolic rate and a fast reproductive cycle, and Costa [30], who reported shortened oocyte development in tropical warm water fishes. Lowerre-Barbieri et al. [38] reported faster oocyte development in tropical fishes. Holden and Raitt [56] reported that batch spawners release eggs in multiple bouts over a prolonged period, ranging from weeks to several months, with spawning costs accounting for approximately 2% of body weight [56]. Similarly, Hunter et al. [48] reported that the energetic cost of spawning reflects a substantial physiological investment required for repeated reproductive events. This batch-spawning pattern is further supported by comparing the relative percentages of advanced vitellogenic oocytes (Vtg3) between fish with and without signs of spawning. Spawned females consistently exhibited multiple oocyte stages along with POFs, indicating continuous oocyte recruitment. The simultaneous presence of fully grown oocytes and POFs within the past 12 to 48 h strongly supports a batch-spawning pattern, as described by Hunter [22] and Murua et al. [5]. Similar spawning patterns were reported in darters by Heins and Baker [57] and Weddle and Burr [58]. Latour et al. [33] also noted that batch spawners typically exhibit multiple oocyte stages in histological sections. In contrast, nonspawned females showed higher proportions of advanced vitellogenic (Vtg3) oocytes without POFs, suggesting retention of a reserve batch for future spawning, consistent with the observations of Schismenou et al. [59]. Thus, the batch spawning and continuous recruitment in pearlspot, likely reflect adaptation to

its tropical habitat and consistently warm conditions influenced by its tropical habitat. In the present study, oocyte diameter increased exponentially across oocyte development stages in spawning-capable ovaries, reflecting the oocyte recruitment pattern in *E. suratensis*. Similar exponential oocyte growth has been reported in *C. edentulus, C. spilopterus, S. brasiliensis, S. rastrifer* and *M. americanus* by Costa [30]. Wallace and Selman [39] noted that oocyte growth in teleosts is regulated primarily by environmental cues and hormonal mechanisms. The observed exponential relationships likely result from the rapid inclusion of vitellogenin during vitellogenesis, leading to yolk granule formation and a sharp increase in the oocyte size, as described in Refs. [44, 60]. During early development, oocyte diameter increases slowly, followed by a rapid acceleration during vitellogenesis, reflecting the biological process of yolk accumulation. This growth pattern is characteristic of asynchronous species such as pearlspot, in which oocytes mature at different rates and multiple oocyte developmental stages coexist within the ovary.

The oocyte size frequency distribution revealed multiple overlapping cohorts, indicating asynchronous oocyte development in pearlspot. This pattern was validated using a GMM, which identified distinct clusters corresponding to successive developmental stages. The coexistence of multiple cohorts supports continuous oocyte recruitment and confirms the presence of a batch-spawning strategy. A similar GMM-based approach was applied by Latour et al. [33] in the indeterminate batch spawner Atlantic menhaden (*Brevoortia tyrannus*), to identify the minimum size of advanced vitellogenic oocytes (Vtg3) for estimating batch fecundity.

The logistic regression model revealed phase-specific variations in the oocyte size at recruitment into vitellogenesis. As the spawning season progressed, a decline in the diameter of advanced vitellogenic oocytes was observed, indicating rapid recruitment of early vitellogenic oocytes into the standing stock. Similar reductions in clutch oocyte size with successive spawning events have been reported in batch-spawning species such as *M. merluccius* [50] and *Thunnus albacores* [24]. Spawning-capable females with Vtg3 oocytes exhibited larger recruitment sizes, indicating that these individuals had not yet spawned and were still accumulating vitellogenic oocytes. In contrast, spawning-capable females with POFs showed smaller recruitment sizes, reflecting repeated spawning and rapid oocyte recruitment during the spawning season. Females at the GVM stage exhibited intermediate recruitment sizes because the mature oocyte batch had already separated from the vitellogenic pool and progressed towards ovulation. This separation likely triggered the early recruitment of the next cohort of previtellogenic oocytes into vitellogenesis, resulting in recruitment at a smaller oocyte size. Costa [30] also noted that recruitment size varies with ovarian phase and spawning timing. These phase-dependent shifts in recruitment size indicate a dynamic fecundity strategy, enabling pearlspot to sustain repeated spawning and maintain reproductive output throughout an extended breeding season.

5 | Conclusion

The present study demonstrates that *E. suratensis* exhibits asynchronous ovarian development, batch spawning and indeterminate fecundity, characterized by continuous oocyte recruitment throughout an extended spawning season. The presence of multiple oocyte cohorts, phase-specific shifts in recruitment size, and the separation of mature oocytes at the GVM stage collectively indicate a flexible reproductive strategy that supports repeated spawning. GMM and logistic regression further confirmed dynamic oocyte development patterns linked to ovarian phase and spawning progression. This reproductive strategy likely represents an adaptive response to the consistently warm conditions of its tropical habitat, enabling sustained reproductive output through rapid oocyte recruitment and short interspawning intervals.

These findings provide valuable insights into the timing of oocyte recruitment, vitellogenesis and atresia, which are essential for optimizing broodstock management, spawning induction and seed production under hatchery conditions. This baseline study also provides a foundation for future research to explore the effects of environmental modifications, hormonal induction and an appropriate feeding strategy model for regulating oocyte recruitment patterns under captive conditions for this economically important species.

Acknowledgements

The first author sincerely acknowledges the Indian Council for Cultural Relations (ICCR), Government of India, for awarding a doctoral research scholarship under the ICCR Fellowship Programme for Foreign Students. The authors are grateful to the Director, School of Industrial Fisheries, Cochin University of Science and Technology, Kochi-16, Kerala, India, for providing all necessary support for this research work. The authors are also grateful to the Department of Marine Biology, Microbiology and Biochemistry, School of Marine Science, for facilitating microscopic work and the National Centre for Aquatic Animal Health for additional support. The authors are also grateful to the DDRC Lab for providing facilities for histological processing and slide preparation. I would like to thank Mr. Deepu Antony for managing cage-cultured fish and assisting with monthly sampling.

Funding

No funding was received for conducting this study.

Ethics Statement

All methods were carried out in accordance with the applicable guidelines of the Committee for the Purpose of Control and Supervision of Experiments on Animals (CPCSEA). The study was approved by the Research Committee of the School of Industrial Fisheries, Cochin University of Science and Technology.

Conflicts of Interest

The authors declare no conflicts of interest.

Data Availability Statement

The data that support the findings of this study are available from the corresponding author upon reasonable request.

References

1. T. V. Arun Kumar, M. A. Pradeep, E. Arshad, and K. K. Vijayan, "Transcriptomic Approach to Study Salinity Tolerance in Euryhaline Cichlid, *Etroplus suratensis* (Bloch, 1790)," *Journal of the Marine Biological Association of India* 62, no. 1 (2020): 24–32, https://doi.org/10.6024/jmbai.2020.62.1.2200-02.

2. G. Biswas, T. K. Ghoshal, M. Natarajan, et al., "Effects of Stocking Density and Presence or Absence of Soil Base on Growth, Weight Variation, Survival and Body Composition of Pearlspot, *Etroplus*

suratensis (Bloch) Fingerlings," *Aquaculture Research* 44, no. 8 (2013): 1266–1276, https://doi.org/10.1111/j.1365-2109.2012.03132.x.

3. S. R. Yadav, B. R. Chavan, N. K. Chadha, S. D. Naik, K. K. Krishnani, and P. B. Sawant, "Effect of Stocking Density on Growth Performance, Plankton Abundance, Body Composition and Haematological Parameters of *Etroplus suratensis* (Bloch, 1790)," *Aquaculture Research* 52, no. 10 (2021): 4752–4766, https://doi.org/10.1111/are.15309.

4. J. Cerdà, M. Fabra, and D. Raldúa, "Physiological and Molecular Basis of Fish Oocyte Hydration," in *The Fish Oocyte: From Basic Studies to Biotechnological Applications* (Dordrecht: Springer Netherlands, 2007), 349–396.

5. H. Murua, G. Kraus, F. Saborido-Rey, P. R. Witthames, A. Thorsen, and S. Junquera, "Procedures to Estimate Fecundity of Marine Fish Species in Relation to Their Reproductive Strategy," *Journal of Northwest Atlantic Fishery Science* 33 (2003): 33–54, https://doi.org/10.2960/j.v33.a3.

6. H. Murua and F. Saborido-Rey, "Female Reproductive Strategies of Marine Fish Species of the North Atlantic," *Journal of Northwest Atlantic Fishery Science* 33 (2003): 23–31, https://doi.org/10.2960/j.v33.a2.

7. G. Plaza, H. Sakaji, H. Honda, Y. Hirota, and K. Nashida, "Spawning Pattern and Type of Fecundity in Relation to Ovarian Allometry in the Round Herring *Etrumeus teres*," *Marine Biology* 152, no. 5 (2007): 1051–1064, https://doi.org/10.1007/s00227-007-0756-3.

8. M. Grande, H. Murua, I. Zudaire, and M. Korta, "Oocyte Development and Fecundity Type of the Skipjack, *Katsuwonus pelamis*, in the Western Indian Ocean," *Journal of Sea Research* 73 (2012): 117–125, https://doi.org/10.1016/j.seares.2012.06.008.

9. A. Alonso-Fernández, R. Domínguez-Petit, M. Bao, C. Rivas, and F. Saborido-Rey, "Spawning Pattern and Reproductive Strategy of Female Pouting *Trisopterus luscus* (Gadidae) on the Galician Shelf of North-Western Spain," *Aquatic Living Resources* 21, no. 4 (2008): 383–393.

10. E. García-Seoane, A. Bernal, and F. Saborido-Rey, "Reproductive Ecology of the Glacier Lanternfish *Benthosema glaciale*," *Hydrobiologia* 727, no. 1 (2014): 137–149.

11. K. Sukumaran, M. Kailasam, K. Vasagam, R. Subburaj, G. Thiagarajan, and K. K. Vijayan, "Enhancement of Breeding Frequency and Reproductive Performance of Pearlspot *Etroplus suratensis* by Curtailing Parental Care," *Aquaculture* 479 (2017): 352–356, https://doi.org/10.1016/j.aquaculture.2017.06.010.

12. B. Varghese, G. George, and S. Thiruvarasu, "Integrating Indoor and Outdoor Breeding Systems to Achieve Year-Round Seed Production in Pearlspot Cichlid, *Etroplus suratensis*," *Aquaculture Research* 53, no. 18 (2022): 6921–6927, https://doi.org/10.1111/are.16125.

13. B. Mandal, P. B. Sawant, S. Dasgupta, et al., "Deviation of Habitat Salinity During Seasonal Gonad Recrudescence Affects Plasma Sex Steroid Levels and Suppresses Gonadal Maturation in an Euryhaline Fish *Etroplus suratensis*," *Aquaculture Research* 48, no. 12 (2017): 5973–5983, https://doi.org/10.1111/are.13422.

14. K. Roshni, C. R. Renjithkumar, and B. M. Kurup, "Reproductive Biology of the Endemic Fish *Etroplus suratensis* (Cichlidae) From a Tropical Estuary in Southern India," *Journal of Ichthyology* 61, no. 3 (2021): 460–466, https://doi.org/10.1134/s0032945221030097.

15. K. G. Padmakumar, L. Bindu, and P. S. Manu, "Captive Breeding and Seed Production of *Etroplus suratensis* in Controlled Systems," *Asian Fisheries Science* 22, no. 1 (2009): 51–60.

16. L. Bindu, in *Captive Breeding Protocols of Two Potential Cultivable Fishes, Etroplus suratensis (Bloch) and Horabagrus brachysoma (Gunther) Endemic to the Western Ghat Region, Kerala* (Mahatma Gandhi University, 2006).

17. B. Ignatius, S. Joseph, and J. Imelda, "Seed Production and Cage Culture of Pearl Spot (*Etroplus suratensis*) Package of Practices" (2012).

18. T. Hussain, P. A. Patil, J. Antony, K. Sukumaran, M. Kailasam, and P. Mahalakshmi, "Effect of Broodstock Stocking Density and Removal of Eggs From Parent Guard on the Spawning Performance of Pearlspot (*Etroplus suratensis*) Reared in the Brackishwater Cage," *Social Science Research Network* (2022).

19. K. P. Sivakumaran, P. Brown, D. Stoessel, and A. Giles, "Maturation and Reproductive Biology of Female Wild Carp, *Cyprinus carpio*, in Victoria, Australia," *Environmental Biology of Fishes* 68, no. 3 (2003): 321–332, https://doi.org/10.1023/a:1027381304091.

20. N. J. Brown-Peterson, D. M. Wyanski, F. Saborido-Rey, B. J. Macewicz, and S. K. Lowerre-Barbieri, "A Standardized Terminology for Describing Reproductive Development in Fishes," *Marine and Coastal Fisheries* 3, no. 1 (2011): 52–70, https://doi.org/10.1080/19425120.2011.555724.

21. Y. Stratoudakis, M. Bernal, K. Ganias, and A. Uriarte, "The Daily Egg Production Method: Recent Advances, Current Applications and Future Challenges," *Fish and Fisheries* 7, no. 1 (2006): 35–57, https://doi.org/10.1111/j.1467-2979.2006.00206.x.

22. J. R. Hunter, "Fecundity, Spawning and Maturity of Female Dover Sole *Microstomus pacificus*, With an Evaluation of Assumption and Precision," *Fishery Bulletin* 90 (1992): 101–128.

23. M. Jan and I. Ahmed, "Reproductive Biology and Histological Studies of Ovarian Development of *Schizothorax plagiostomus* in River Lidder From Kashmir Himalaya," *Journal of Applied Ichthyology* 35, no. 2 (2019): 512–519, https://doi.org/10.1111/jai.13858.

24. I. Zudaire, H. Murua, M. Grande, et al., "Fecundity Regulation Strategy of the Yellowfin Tuna (*Thunnus albacares*) in the Western Indian Ocean," *Fisheries Research* 138 (2013): 80–88, https://doi.org/10.1016/j.fishres.2012.07.022.

25. G. West, "Methods of Assessing Ovarian Development in Fishes: A Review," *Australian Journal of Marine and Freshwater Research* 41, no. 2 (1990): 199–222, https://doi.org/10.1071/mf9900199.

26. J. Núñez and F. Duponchelle, "Towards a Universal Scale to Assess Sexual Maturation and Related Life History Traits in Oviparous Teleost Fishes," *Fish Physiology and Biochemistry* 35, no. 1 (2009): 167–180.

27. H. J. Grier, M. C. Uribe-Aranzábal, and R. Patiño, "The Ovary, Folliculogenesis, and Oogenesis in Teleosts," in *Reproductive Biology and Phylogeny of Fishes* (CRC Press, 2009), 25–84.

28. J. R. Hunter and J. Macewicz, "Rates of Atresia in the Ovary of Captive and Wild Northern Anchovy; *Engraulis mordax*," *Fishery Bulletin* 83, no. 2 (1985).

29. V. S. Blazer, "Histopathological Assessment of Gonadal Tissue in Wild Fishes," *Fish Physiology and Biochemistry* 26, no. 1 (2002): 85–101, https://doi.org/10.1023/a:1023332216713.

30. E. Costa, *Reproductive Strategies of Marine Fishes From the Southwest Atlantic Ocean: An Application of Histological and Image Processing Techniques* (University of São Paulo, 2015).

31. K. Coward, "Aspects of the Reproductive Biology and Endocrinology of the Substrate-Spawning Cichlid *Tilapia zillii*," *Institute of Aquaculture* (University of Stirling, 1997).

32. P. J. T. Denusta, E. G. De Jesus-Ayson, M. A. Laron, F. A. Aya, and L. M. B. Garcia, "Gonad Development and Size-at-Maturity of Silver Therapon *Leiopotherapon plumbeus*," *Journal of Applied Ichthyology* 35, no. 4 (2019): 933–943.

33. R. J. Latour, J. Gartland, and A. M. Schueller, "The Reproductive Biology and Fecundity of Female Atlantic Menhaden," *Marine and Coastal Fisheries* 15, no. 5 (2023): e210269, https://doi.org/10.1002/mcf2.10269.

34. G. J. McLachlan and D. Peel, *Finite Mixture Models* (John Wiley and Sons, 2000).

35. S. A. Sethi, J. Gerken, and J. Ashline, "Accurate Aging of Juvenile Salmonids Using Fork Lengths," *Fisheries Research* 185 (2017): 161–168, https://doi.org/10.1016/j.fishres.2016.09.012.

36. RStudio Team, *Rstudio: Integrated Development Environment for R* (RStudio PBC, 2020).

37. S. K. Lowerre-Barbieri, N. J. Brown-Peterson, H. Murua, J. Tomkiewicz, D. M. Wyanski, and F. Saborido-Rey, "Emerging Issues and Methodological Advances in Fisheries Reproductive Biology," *Marine and Coastal Fisheries* 3, no. 1 (2011): 32–51, https://doi.org/10.1080/19425120.2011.555725.

38. S. K. Lowerre-Barbieri, K. Ganias, F. Saborido-Rey, H. Murua, and J. R. Hunter, "Reproductive Timing in Marine Fishes: Variability, Temporal Scales, and Methods," *Marine and Coastal Fisheries* 3, no. 1 (2011): 71–91, https://doi.org/10.1080/19425120.2011.556932.

39. R. A. Wallace and K. Selman, "Cellular and Dynamic Aspects of Oocyte Growth in Teleosts," *American Zoologist* 21, no. 2 (1981): 211–231, https://doi.org/10.1093/icb/21.2.325.

40. K. Ganias, "Determining the Indeterminate: Evolving Concepts and Methods on the Assessment of the Fecundity Pattern of Fishes," *Fisheries Research* 138 (2013): 23–30, https://doi.org/10.1016/j.fishres.2012.05.006.

41. B. Stéquert and R. Ramcharrun, "La eproduction du Listao (*Katsuwonus Pelamis*) Dans le Bassin Ouest de L'Océan Indien," *Aquatic Living Resources* 9, no. 3 (1996): 235–247.

42. J. R. Hunter and B. J. Macewicz, "Measurement of Spawning Frequency in Multiple Spawning Fishes," in *An Egg Production Method for Estimating Spawning Biomass of Pelagic Fish*, ed. R. Lasker (NOAA Technical Report, 1985), 79–94.

43. M. Greer Walker, P. R. Witthames, and I. Bautista de los Santos, "Is the Fecundity of the Atlantic Mackerel (*Scomber scombrus*) Determinate?" *Sarsia* 79, no. 1 (1994): 13–26, https://doi.org/10.1080/00364827.1994.10413543.

44. C. R. Tyler and J. P. Sumpter, "Oocyte Growth and Development in Teleosts," *Reviews in Fish Biology and Fisheries* 6, no. 3 (1996): 287–318, https://doi.org/10.1007/bf00122584.

45. D. A. Pavlov and N. G. Emel'Yanova, "Reproductive Dynamics," in *Fish Reproductive Biology* (2016), 50–97.

46. M. Korta, in *New Methodologies Applied to Quantify the Dynamics of the Ovary in Indeterminate Fecundity Species* (University of the Basque Country, 2010).

47. R. S. McBride, S. Somarakis, G. R. Fitzhugh, et al., "Energy Acquisition and Allocation to Egg Production in Relation to Fish Reproductive Strategies," *Fish and Fisheries* 16, no. 1 (2015): 23–57, https://doi.org/10.1111/faf.12043.

48. J. R. Hunter and B. J. Macewicz, "The Spawning Frequency of Skipjack Tuna, *Katsuwonus pelamis*, from the South Pacific," *Fishery Bulletin* 84, no. 4 (1990).

49. N. J. Brown-Peterson, R. T. Leaf, A. M. Schueller, and M. J. Andres, "Reproductive Dynamics of Gulf Menhaden (*Brevoortia patronus*) in the Northern Gulf of Mexico," *Fishery Bulletin* 115, no. 3 (2017): 284–299, https://doi.org/10.7755/fb.115.3.2.

50. H. Murua and L. Motos, "Reproductive Strategy and Spawning Activity of the European Hake *Merluccius merluccius* in the Bay of Biscay," *Journal of Fish Biology* 69, no. 5 (2006): 1288–1303, https://doi.org/10.1111/j.1095-8649.2006.01169.x.

51. S. S. Guraya, *The Cell and Molecular Biology of Fish Oogenesis* (Karger, 1986).

52. D. C. Heins and N. J. Brown-Peterson, "The Reproductive Biology of Small Fishes and the Clutch Concept," *Aquaculture, Fish and Fisheries* 2, no. 4 (2022): 253–264.

53. K. Ganias, S. Somarakis, A. Machias, and A. Theodorou, "Pattern of Oocyte Development and Batch Fecundity in the Mediterranean Sardine," *Fisheries Research* 67, no. 1 (2004): 13–23, https://doi.org/10.1016/j.fishres.2003.08.008.

54. M. Yoneda, H. Kitano, S. Selvaraj, M. Matsuyama, and A. Shimizu, "Dynamics of Gonadosomatic Index of Fish With Indeterminate Fecundity," *Marine Biology* 160, no. 10 (2013): 2733–2741, https://doi.org/10.1007/s00227-013-2266-9.

55. T. Fish, N. Wolf, B. P. Harris, and J. V. Planas, "A Comprehensive Description of Oocyte Developmental Stages in Pacific Halibut," *Journal of Fish Biology* 97, no. 6 (2020): 1880–1885, https://doi.org/10.1111/jfb.14551.

56. M. J. Holden and D. F. S. Raitt, eds., *Manual of Fisheries Science* (FAO, 1979), 211.

57. D. C. Heins and J. A. Baker, "Clutch Production in the Darter *Etheostoma lynceum*," *Journal of Fish Biology* 42, no. 6 (1993): 819–829, https://doi.org/10.1111/j.1095-8649.1993.tb00392.x.

58. G. K. Weddle and B. M. Burr, "Fecundity and the Dynamics of Multiple Spawning in Darters," *Copeia* 1991, no. 2 (1991): 419–433, https://doi.org/10.2307/1446591.

59. E. Schismenou, S. Somarakis, A. Thorsen, and O. S. Kjesbu, "Dynamics of de Novo Vitellogenesis in Fish With Indeterminate Fecundity," *Marine Biology* 159, no. 4 (2012): 757–768, https://doi.org/10.1007/s00227-011-1852-y.

60. R. Patiño and C. V. Sullivan, "Ovarian Follicle Growth, Maturation, and Ovulation in Teleost Fish," *Fish Physiology and Biochemistry* 26, no. 1 (2002): 57–70.